Symbiosis

www.symbiosisonline.org
www.symbiosisonlinepublishing.com

Research Article International Journal of Molecular and Theoretical Physics Open Access

Structural Geometry, Vibrational and Electronic Spectra Investigation on Naringin Molecule Using Experimental and Density functional theory calculation

Suresh R[1], Balakumar R[1], Krishnakumar N[2], Saleem H[2*] and Subashchandrabose S[1, 3*]

[1]*Centre for Research and Development, PRIST University, Thanjavur, Tamilnadu, India-613403*

[2]*Department of Physics, Annamalai University, Annamalai nagar, Tamil Nadu, India-608 002.*

[3]*Centre for Functionalized Magnetic materials (FunMagMa), Immanuel Kant Baltic Federal University-236000, Kaliningrad, Russia.*

Received: February 8, 2018; Accepted: February 24, 2018; Published: March 1, 2018

***Corresponding author:** S. Subashchandrabose, Centre for Research and Development, PRIST University, Thanjavur, Tamilnadu, India-613403. Tel: +91 9976853476; E-mail: sscbphysics@gmail.com*

Abstract

In the present investigation we investigate the structural, spectral and Molecular Orbitals (MO's) properties of Naringin compound. It is a bioflavonoid, present in the fruits; it is responsible for bitter taste in fruits. The Naringin has a flavanone-7-O-glycoside between the flavanone naringenin and the disaccharide neohesperidose. It consists of naringenin (ring A-C), D-glucose (ring D) and L-rhamnose (ring E). Our aim is to predict the molecular structure and investigate the insights of the Naringin molecule. Besides that to study the vibrational behavior of Naringin, the FT-IR and FT-Raman spectra were recorded in the ranges of 4000-400cm^{-1} and 3500-50cm^{-1} respectively, and to study the frontier molecular orbitals, the UV-Visible spectrum was recorded in the range of 500-200nm. In addition to that the geometry of Naringin molecular structure was optimized by Density Functional Theory (DFT/B3LYP) calculation using 6-31g (d, p) level of basis set. For the optimized structure, vibrational spectral calculation was performed by the same level of theory calculation, furthermore, interpreted the calculated spectra of Naringin in terms of TED analysis. Moreover, to explain the inter and intra molecular charge transfer within the molecule the Natural Bond Orbital analysis (NBO) was performed, NBO analysis gave us a clear picture about hyperconjugative interaction energy between the donor (i) and acceptor(j) bond orbitals. In addition to that, the first order hyperpolarizability (β0), polarizability (α) and dipole moment (μ) of Naringin was computed. The frontier MO's (HOMO-LUMO) of Naringin was analyzed by TD-B3LYP/6-31g (d, p) level of basis set. Finally, the experimentally recorded results were compared with computed values, the agreement and discrepancies were studied carefully.

Keywords: FT-IR; FT-Raman; TED; NBO; Naringin;

Introduction

Flavonoids are naturally occurring phenolic compounds with a diverse range of bioactivities [1]. Among flavonoids, Naringin has great potential especially in the food and pharmaceutical industries due to their recognized antioxidant, anti-inflammatory, anti-ulcer, and hypocholesterolemic effects, whereas the Naringenin has also shown anti-mutagenic and neuroprotective activities [2]. Naringin is a 'flavanone glycoside found in grape and citrus fruits. It has the distinct bitter taste of grapefruit juice. Its molecular formula is C27H32O14 and molecular weight is about 580.4g/mol, it consists of L-rhamnose and D-glucose with Naringenin at the 7-carbon portion [3]. It is moderately soluble in water [4]. It has been reported to protect against oxygen free radical-stimulated K_ permeability [5], metal chelating, antioxidant and free radical scavenging properties [6], Naringin, a major bioflavonoid in grapefruit, it has been shown to reduce radiation-induced damage to DNA [7]. It also acts as the inhibitor of VEGF (Vascular Endothelial Growth Factor) release, which causes angiogenesis and has been proven to be effective against ethanol injury in rats [8, 9].

Since the Naringin flavonoid having a wide application in above-mentioned fields, we investigate the structure geometry, vibrational spectra, Frontier Molecular Orbitals (FMOs), inter and intramolecular interactions by (experimental and computation) methods such as FT-IR, FT-Raman, UV-Visible spectra, DFT and Time dependent-DFT calculations. To the best of our knowledge, there is no such an article being published till now.

Experimental Details

FT-Raman and FT-IR Spectra

The solid form of Naringin compound was purchased from sigma Aldrich Company USA. The FT-Raman spectra was recorded in the region 3500-50cm^{-1} using the FT-Raman spectrometer with Nd:YAG laser source, and 1064nm as a excitation wavelength with spectral resolution of 4cm^{-1} on a Bruker model IFS66V spectrophotometer equipped with an FRA 106 FT-Raman module accessory. The spectral measurements were carried out at Sree Chitra Tirunal Institute for Medical Sciences and Technology, Poojappura, Thiruvananthapuram, Kerala, India. The FT-IR spectrum of this compound was recorded in the region 400-4000 cm^{-1} on an IFS 66V spectrophotometer

 * ***Corresponding author email:*** *sscbphysics@gmail.com*

using the KBr pellet technique. The spectrum was recorded at room temperature, with a scanning speed of 10 cm^{-1} per minute and at the spectral resolution of 2.0 cm^{-1} in CSIL Laboratory, Annamalai University, and Tamilnadu, India. The ultraviolet absorption spectrum of Naringin was recorded in the range of 200-500 nm using a shimadzu UV-2401PC, UV-Visible recording spectrometer. The UV pattern is taken from a 10^{-5} molar solution of Naringin dissolved in methanol.

Computational Details

The entire calculations were performed at DFT level on a Pentium 1V/3.02 GHz personal computer using Gaussian 03W Program package [10], invoking gradient geometry optimization [11]. In this study, the DFT/B3LYP/6-31G (d, p) method has been utilized for the computation of molecular structure, vibrational frequencies and energies of optimized structures. By combining the results of the GAUSSVIEW program with symmetry considerations, vibrational frequency assignments were made with a high degree of accuracy and also the scaled quantum mechanics calculation was used to identify the vibrations [12, 13].

It should be noted that Gaussian 03W package able to calculate the Raman activity. The Raman activities were transformed into Raman intensities using Raint program by the expression [14]:

$$I_i = 10^{-12} \times (v_0 - v_i)^4 \times \frac{1}{v_i} \times RA_i \qquad (1)$$

Where Ii is the Raman intensity, RA_i is the Raman scattering activities, νi is the wavenumber of the normal modes and ν0 denotes the wavenumber of the excitation laser [15].

Results and Discussion

Molecular Geometry

Molecular structure of the Naringin was optimized by using DFT/B3LYP level of theory calculation using 6-31G (d, p) basis set. The optimized molecular structure along with numbering scheme is given in Figure 1. It is belongs to C_1 point group symmetry. To the best of our literature survey, the crystal data of this molecule is not available till date [16]. So that, the optimized geometric parameters of Naringin is compared with Naringenin, quercetin and some flavones. It consists of L-rhamnose and D-glucose with naringenin at the 7-carbon, Naringin structure has 8 hydroxyl groups; it leads the molecule more inter-molecular hydrogen bonding interactions. The carbonyl present in naringenin forms intra-molecular hydrogen bonding interaction between carbonyl and hydroxyl groups. Due to this, the bond lengths of C_3-C_8 (1.424), C_8-C_{10} (1.398) in ring A and C_4-C_5 (1.516 Å) in ring B are positively elongated with C-C bond lengths (~1.4 Å) in ring C as well as with literature values [16].

Zhang et al. observed the C=O and C-O bond lengths are about 1.235 and 1.427 Å, respectively for 5, 6, 7, 4'-tetramethoxy isoflavone [17]. These observed values are in line with the calculated values (C_4=O_{14}: 1.243 and C_8-O_{15}: 1.337Å) of Naringin molecule. Moreover, there is a shrink in bond length of C_8-O_{15} due to delocalization of π-electron from C_4=O_{14}. On comparing the C-C bond length in ring D, E with ring A, B and C are higher (~1.5 Å) due to the boat form of ring D and ring E. In ring A, the angle of C_8-O_{15}-H_{16} and C_3-C_8-C_{10} are about 106.52º and 120.74º respectively. These angles are negatively deviated from the angles of C_{24}-O_{27}-H_{28} (109.21º) and C_{22}-C_{24}-C_{20} (119.78º) is due to the electron localized in ring E. The calculated bond lengths, bond angles and dihedral angles are listed in Table S1 (Supporting information).

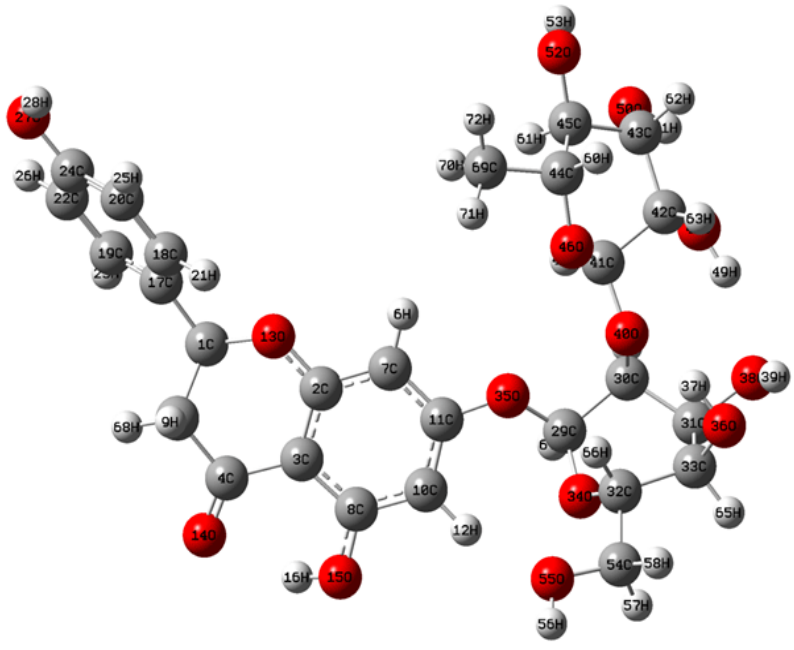

Figure 1: Optimized Molecular structure of Naringin.

Table S1: The optimized bond lengths, bond angles and dihedral angles of Naringin using B3LYP/6-31G(d,p) basis set.

Parameters	B3LYP/6-31G(d,p)	Exp.	Parameters	B3LYP/6-31G(d,p)	Exp.
Bond lengths (Å)			**Bond length Contd...**		
C_1-C_5	1.533		C_{30}-O_{40}	1.427	
C_1-O_{13}	1.447	1.376	C_{30}-H_{59}	1.094	
C_1-C_{17}	1.509	1.467	C_{31}-C_{33}	1.555	
C_1-H_{73}	1.100		C_{31}-O_{38}	1.424	
C_2-C_3	1.420	1.386	C_{31}-H_{64}	1.095	
C_2-C_7	1.385	1.388	C_{32}-C_{33}	1.544	
C_2-O_{13}	1.361	1.365	C_{32}-O_{34}	1.442	
C_3-C_4	1.447	1.449	C_{32}-C_{54}	1.521	
C_3-C_8	1.424	1.406	C_{32}-H_{66}	1.097	
C_4-C_5	1.516	1.455	C_{33}-O_{36}	1.428	
C_4-O_{14}	1.243	1.238	C_{33}-H_{65}	1.095	
C_5-H_9	1.098		O_{36}-H_{37}	0.974	
C_5-H_{68}	1.093		O_{38}-H_{39}	0.977	
H_6-C_7	1.083	0.930	O_{40}-C_{41}	1.443	
C_7-C_{11}	1.404	1.378	C_{41}-C_{42}	1.536	
C_8-C_{10}	1.398	1.364	C_{41}-O_{46}	1.394	
C_8-O_{15}	1.337	1.355	C_{41}-H_{47}	1.095	
C_{10}-C_{11}	1.398	1.399	C_{42}-C_{43}	1.529	
C_{10}-H_{12}	1.081	0.930	C_{42}-O_{48}	1.418	
C_{11}-O_{35}	1.368		C_{42}-H_{63}	1.100	
O_{14}-H_{16}	1.685		C_{43}-C_{45}	1.550	
O_{15}-H_{16}	0.995	0.910	C_{43}-O_{50}	1.422	
C_{17}-C_{18}	1.399	1.389	C_{43}-H_{62}	1.101	
C_{17}-C_{19}	1.400	1.392	C_{44}-C_{45}	1.539	
C_{18}-C_{20}	1.393	1.383	C_{44}-O_{46}	1.437	
C_{18}-H_{21}	1.085	0.930	C_{44}-H_{60}	1.100	
C_{19}-C_{22}	1.391	1.377	C_{44}-C_{69}	1.519	
C_{19}-H_{23}	1.087	0.930	C_{45}-O_{52}	1.424	
C_{20}-C_{24}	1.400	1.385	C_{45}-H_{61}	1.099	
C_{20}-H_{25}	1.088	0.930	O_{48}-H_{49}	0.978	
C_{22}-C_{24}	1.399	1.376	O_{50}-H_{51}	0.970	
C_{22}-H_{26}	1.085	0.930	O_{52}-H_{53}	0.966	
C_{24}-O_{27}	1.365		C_{54}-O_{55}	1.412	
O_{27}-H_{28}	0.966		C_{54}-H_{57}	1.103	
C_{29}-C_{30}	1.549		C_{54}-H_{58}	1.095	
C_{29}-O_{34}	1.410		O_{55}-H_{56}	0.968	

C_{29}-O_{35}	1.412		C_{69}-H_{70}	1.095	
Bond lengths (Å)			**Bond lengths (Å)**		
C_{29}-H_{67}	1.096		C_{69}-H_{71}	1.092	
C_{30}-C_{31}	1.534		C_{69}-H_{72}	1.093	
Bond Angles (°)			**Bond Angles (°)**		
C_5-C_1-O_{13}	109.96	120.85	C_{17}-C_{19}-C_{22}	121.24	
C_5-C_1-C_{17}	113.40	128.80	C_{17}-C_{19}-H_{23}	119.67	
C_5-C_1-H_{73}	108.54		C_{22}-C_{19}-H_{23}	119.09	
O_{13}-C_1-C_{17}	108.05	111.15	C_{18}-C_{20}-C_{24}	120.00	
O_{13}-C_1-H_{73}	107.39		C_{18}-C_{20}-H_{25}	120.02	
C_{17}-C_1-H_{73}	109.33		C_{24}-C_{20}-H_{25}	119.98	
C_3-C_2-C_7	121.19	121.70	C_{19}-C_{22}-C_{24}	119.62	
C_3-C_2-O_{13}	121.41	122.03	C_{19}-C_{22}-H_{26}	121.37	
C_7-C_2-O_{13}	117.40	116.03	C_{24}-C_{22}-H_{26}	119.01	
C_2-C_3-C_4	120.71	119.12	C_{20}-C_{24}-C_{22}	119.78	
C_2-C_3-C_8	118.46	118.52	C_{20}-C_{24}-O_{27}	122.78	
C_4-C_3-C_8	120.66	122.33	C_{22}-C_{24}-O_{27}	117.44	
C_3-C_4-C_5	115.78	115.93	C_{24}-O_{27}-H_{28}	109.21	
C_3-C_4-O_{14}	123.06		C_{30}-C_{29}-O_{34}	112.11	
C_5-C_4-O_{14}	121.13		C_{30}-C_{29}-O_{35}	107.21	
C_1-C_5-C_4	111.08	122.03	C_{30}-C_{29}-H_{67}	109.79	
C_1-C_5-H_9	109.46		O_{34}-C_{29}-O_{35}	112.95	
C_1-C_5-H_{68}	110.97		O_{34}-C_{29}-H_{67}	104.98	
C_4-C_5-H_9	108.41		O_{35}-C_{29}-H_{67}	109.80	
C_4-C_5-H_{68}	109.43		C_{29}-C_{30}-C_{31}	108.12	
H_9-C_5-H_{68}	107.38		C_{29}-C_{30}-O_{40}	112.41	
C_2-C_7-C_6	121.16		C_{29}-C_{30}-H_{59}	108.86	
C_2-C_7-C_{11}	118.76	118.72	C_{31}-C_{30}-O_{40}	107.36	
C_6-C_7-C_{11}	120.06		C_{31}-C_{30}-H_{59}	110.16	
C_3-C_8-C_{10}	120.74	120.20	O_{40}-C_{30}-H_{59}	109.91	
C_3-C_8-O_{15}	120.54	121.20	C_{30}-C_{31}-C_{33}	108.94	
C_{10}-C_8-O_{15}	118.71	116.80	C_{30}-C_{31}-O_{38}	111.22	
C_8-C_{10}-C_{11}	118.63	120.35	C_{30}-C_{31}-H_{64}	109.10	
C_8-C_{10}-H_{12}	118.62		C_{33}-C_{31}-O_{38}	109.57	
C_{11}-C_{10}-H_{12}	122.70		C_{33}-C_{31}-H_{64}	109.72	
C_7-C_{11}-C_{10}	122.22	120.48	O_{38}-C_{31}-H_{64}	108.27	
C_7-C_{11}-O_{35}	114.01		C_{33}-C_{32}-O_{34}	109.67	
C_{10}-C_{11}-O_{35}	123.77		C_{33}-C_{32}-C_{54}	113.78	

C_1-O_{13}-C_2	116.59	120.85	C_{33}-C_{32}-H_{66}	109.20	
C_8-O_{15}-H_{16}	106.52		O_{34}-C_{32}-C_{54}	105.99	
Bond Angles (°)			**Bond Angles (°)**		
C_1-C_{17}-C_{18}	121.16		O_{34}-C_{32}-H_{66}	109.00	
C_1-C_{17}-C_{19}	120.24	122.71	C_{54}-C_{32}-H_{66}	109.07	
C_{18}-C_{17}-C_{19}	118.55	117.19	C_{31}-C_{33}-C_{32}	110.36	
C_{17}-C_{18}-C_{20}	120.80	119.30	C_{31}-C_{33}-O_{36}	109.48	
C_{17}-C_{18}-H_{21}	119.55		C_{31}-C_{33}-H_{65}	109.20	
C_{20}-C_{18}-H_{21}	119.64		C_{32}-C_{33}-O_{36}	111.44	
C_{32}-C_{33}-H_{65}	110.90		C_{32}-C_{54}-O_{55}	112.01	
O_{36}-C_{33}-H_{65}	105.31		C_{32}-C_{54}-H_{57}	108.61	
C_{29}-O_{34}-C_{32}	114.52		C_{32}-C_{54}-H_{58}	108.86	
C_{11}-O_{35}-C_{29}	119.78		O_{55}-C_{54}-H_{57}	111.97	
C_{33}-O_{36}-H_{37}	105.12		O_{55}-C_{54}-H_{58}	107.36	
C_{31}-O_{38}-H_{39}	104.36		H_{57}-C_{54}-H_{58}	107.91	
C_{30}-O_{40}-C_{41}	116.34		C_{54}-O_{55}-H_{56}	106.57	
O_{40}-C_{41}-C_{42}	108.94		C_{44}-C_{69}-H_{70}	110.15	
O_{40}-C_{41}-O_{46}	108.38		C_{44}-C_{69}-H_{71}	109.57	
O_{40}-C_{41}-H_{47}	107.95		C_{44}-C_{69}-H_{72}	110.51	
C_{42}-C_{41}-O_{46}	113.73		H_{70}-C_{69}-H_{71}	109.00	
C_{42}-C_{41}-H_{47}	109.52		H_{70}-C_{69}-H_{72}	108.38	
O_{46}-C_{41}-H_{47}	108.15		H_{71}-C_{69}-H_{72}	109.20	
C_{41}-C_{42}-C_{43}	110.15		C_{32}-C_{54}-O_{55}	112.01	
C_{41}-C_{42}-O_{48}	110.63		C_{32}-C_{54}-H_{57}	108.61	
C_{41}-C_{42}-H_{63}	108.33		C_{32}-C_{54}-H_{58}	108.86	
C_{43}-C_{42}-O_{48}	107.85		O_{55}-C_{54}-H_{57}	111.97	
C_{43}-C_{42}-H_{63}	108.91		O_{55}-C_{54}-H_{58}	107.36	
O_{48}-C_{42}-H_{63}	110.96		H_{57}-C_{54}-H_{58}	107.91	
C_{42}-C_{43}-C_{45}	111.34		C_{54}-O_{55}-H_{56}	106.57	
C_{42}-C_{43}-$_{50}$	109.69		C_{44}-C_{69}-H_{70}	110.15	
C_{42}-C_{43}-H_{62}	108.26		C_{44}-C_{69}-H_{71}	109.57	
C_{45}-C_{43}-$_{50}$	108.45		C_{44}-C_{69}-H_{72}	110.51	
C_{45}-C_{43}-H_{62}	108.29		H_{70}-C_{69}-H_{71}	109.00	
$_{50}$-C_{43}-H_{62}	110.82		H_{70}-C_{69}-H_{72}	108.38	
C_{45}-C_{44}-O_{46}	109.80		H_{71}-C_{69}-H_{72}	109.20	
C_{45}-C_{44}-H_{60}	107.84		**Dihedral angles (º)**		
C_{45}-C_{44}-C_{69}	112.91		O_{13}-C_1-C_5-C_4	-54.56	
O_{46}-C_{44}-H_{60}	110.48		O_{13}-C_1-C_5-H_9	65.13	

O_{46}-C_{44}-C_{69}	106.72		O_{13}-C_1-C_5-H_{68}	-176.53	
H_{61}-C_{44}-C_{69}	109.10		C_{17}-C_1-C_5-C_4	-175.65	
C_{43}-C_{45}-C_{44}	111.98		C_{17}-C_1-C_5-H_9	-55.96	
Bond angles (Å)			**Dihedral angles (º)**		
C_{43}-C_{45}-O_{52}	112.34		C_{17}-C_1-C_5-H_{68}	62.38	
C_{43}-C_{45}-H_{61}	106.70		H_{73}-C_1-C_5-C_4	62.65	
C_{44}-C_{45}-O_{52}	105.67		H_{73}-C_1-C_5-H_9	-177.67	
C_{44}-C_{45}-H_{61}	108.62		H_{73}-C_1-C_5-H_{68}	-59.33	
O_{52}-C_{45}-H_{61}	111.54		C_5-C_1-O_{13}-C_2	51.63	
C_{41}-O_{46}-C_{44}	117.45		C_{17}-C_1-O_{13}-C_2	175.88	
C_{42}-O_{48}-H_{49}	108.56		H_{73}-C_1-O_{13}-C_2	-66.28	
C_{43}-$_{50}$-H_{51}	105.73		C_5-C_1-C_{17}-C_{18}	80.31	
C_{45}-O_{52}-H_{53}	107.93		C_5-C_1-C_{17}-C_{19}	-97.28	
Exp. – Experimental					

Vibrational Assignments

The Naringin molecule contains 73 atoms (including 8 –OH group, one methylene and methyl groups); hence it can have 213 normal modes of vibrations. To the best of our knowledge, there is no complete vibrational spectroscopic study carried out on Naringin. In the present investigation the FT-IR and FT-Raman spectra were recorded in the region of 4000-400cm^{-1} and 3500-50cm^{-1}, respectively. Stimulated IR and Raman spectra were constructed and compared with experimental spectra. The combined spectrum of FT-IR showed in Figure 2 and the FT-Raman spectrum showed in Figure 3. Similarly, Observed frequencies and calculated wave numbers are compared and listed in Table 1, also provided a detail results in Table S2 (Supporting information). The frequency calculation was performed by using B3LYP level of theory using 6-31G (d, p) basis set. The TED for all fundamental vibrations is calculated using SQM method.

C-H Vibrations

The heteroaromatic structure shows the presence of C-H vibration in the region 3100-3000 cm^{-1}, which is the characteristic region for the ready identification of C-H stretching vibration [18]. In this region, the bands are not affected appreciably by nature of the substituent. In the present work, the C-H aromatic stretching frequency observed at 3071 cm^{-1} as a weak band in FT-Raman and its corresponding calculated wavenumber is 3083 cm^{-1} (mode numbers: 202). For the same mode five more harmonic vibrations are also appeared (mode numbers: 200, 201, 203-205). As expected these modes are pure stretching modes as it evident from the TED column (their contribution ~95%). The FT-IR bands 2890-2970 cm^{-1} (weak) and FT-Raman bands 2939, 2958, 2976 cm^{-1} (weak) are assigned to C-H stretching in ring B and ring D respectively. These assignments are comparable with harmonic frequencies 2888, 2939, 2943, 2952, 2965 and 2985 cm^{-1} (mode numbers: 185, 191, 193-196) and also find support from TED. The mode numbers: 183, 184, 186, 188 and 192 are

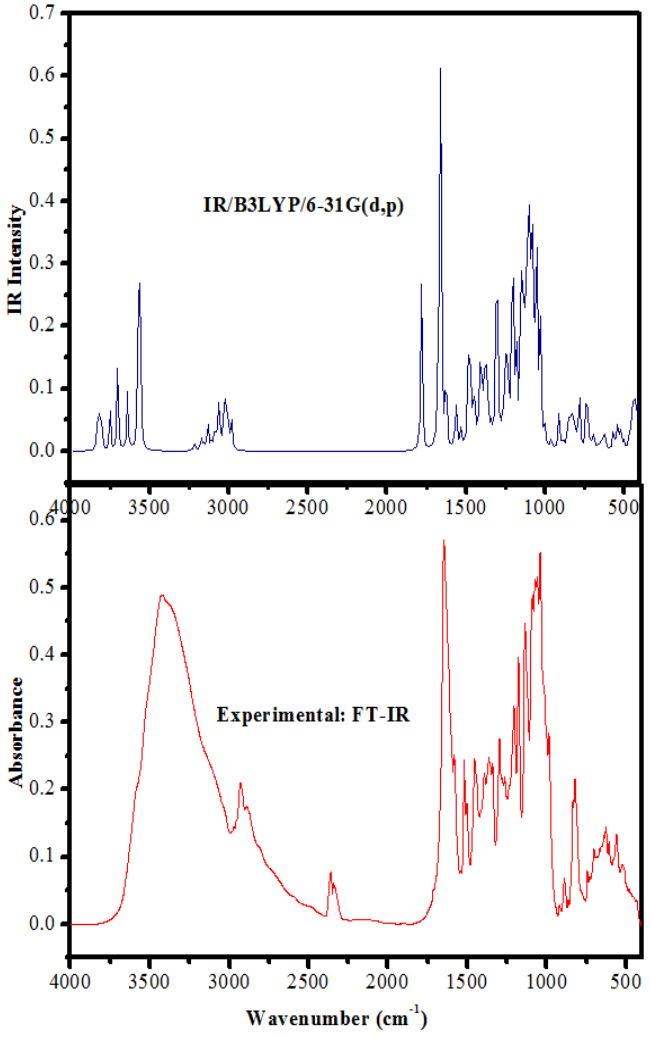

Figure 2: The combined experimental and theoretical FT-IR spectra of Naringin.

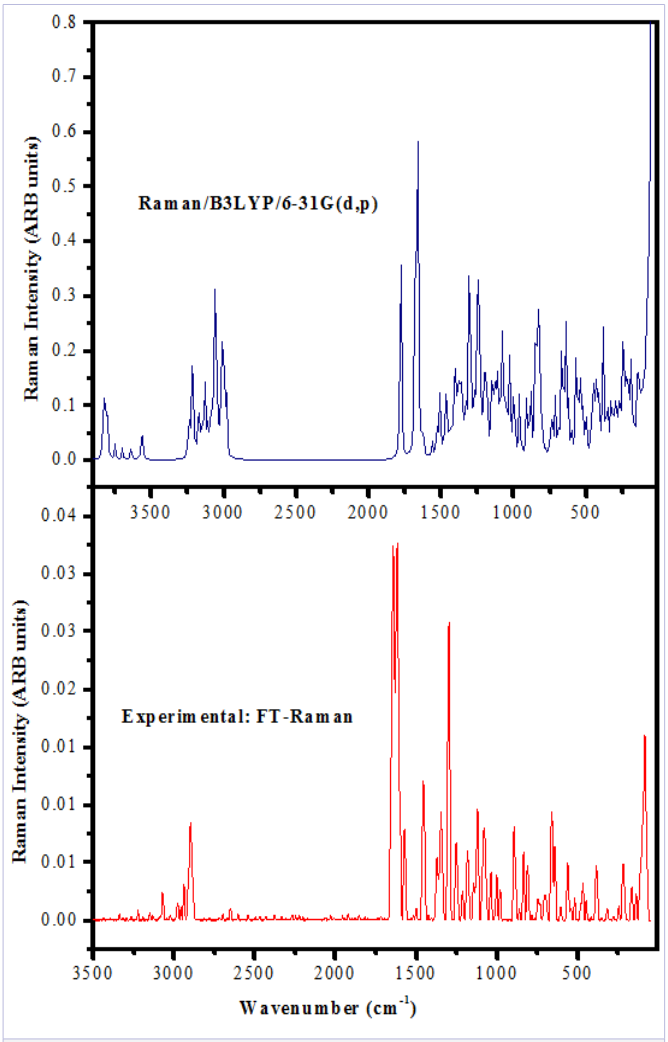

Figure 3: The combined experimental and theoretical FT-Raman spectra of Naringin.

assigned to ν_{C-H} in ring E. The in-plane bending of C-H is observed at 1089, 1178 and 1296 (strong) in FT-IR and 1002 cm^{-1} in FT-Raman spectra. The calculated wavenumbers in the range 990-1312 cm^{-1} (mode numbers: 101, 117, 125-128, 140, 143, 145-147) are assigned to δ_{C-H} with considerable TED value. The Out-of-plane bending of τ_{C-H} mode is observed at 896, 812, 607 cm^{-1} in FT-Raman and 919 and 608 cm^{-1} in FT-IR spectra, whereas the harmonic values are in the range of 605-922 cm^{-1} (mode nos: 67, 68, 80-82, 86, 94, 95). These assignments are in agreement with literature values [18-19].

Methyl Group (CH_3) Vibrations

The C-H stretching mode in CH_3 occurs at lower wavenumber than those of the aromatic ring (3000-3100 cm^{-1}). The asymmetric stretching mode of the CH_3 group is expected to occur in the region of 2980 cm^{-1} and the symmetric one is at 2870 cm^{-1} [20-21]. The methyl group (CH_3) has three stretching vibrations, namely one symmetric and two asymmetric modes [22]. In this study, the computed wavenumbers for the CH_3 (asy) stretching and CH_3 (sym) stretching are 3021, 3008 cm^{-1} (mode numbers: 199, 198) and 2938 cm^{-1} /mode no: 190, respectively. These modes are supported by TED and above literature. These modes are 100% (TED) pure for CH_3 stretching vibration.

Two asymmetric CH_3 bending, one symmetric CH_3 bending, two CH_3 rocking and one CH_3 torsional vibrations are possible [22]. The methyl group symmetric deformation absorbs moderately to strong in the range 1365±25 cm^{-1} and asymmetric methyl deformations in the region 1390-1480 cm^{-1} [23]. Based on the above conclusion the observed bands 1453/1456 (FT-IR/Raman) and 1363 cm^{-1}/FT-IR are attributed to δCH_3 (asym) and δCH_3 (sym), respectively. The methyl rocking generally appears in the region 1050±30 and 975+45 cm^{-1} [24], as a weak moderate or sometimes strong band, the wavenumber of which is coupled to the C-C stretching vibrations, which occur in the neighborhood of 900 cm^{-1}. The FT-Raman band 1122 cm^{-1} (medium strong) and

Table S2: The vibrational assignments of Naringin using Scaled Quantum Mechanics method (B3LYP/6-31G(d,p)).

Mode No.	Scaled B3LYP[a]	FT-IR	FT-Raman	I^b_{IR}	I^c_{Raman}	Vibrational assignments TED[d] (≥ 10)
1	3			0.05	79.30	$\tau_{C29-O35-C11-C7}(46)+\tau_{C29-O35-C11-C10}(45)$
2	14			0.00	13.63	$\tau_{C32-O34-C29-O35}(11)+\tau_{C41-O40-C30-C29}(14)$
3	18			0.02	28.67	$\tau_{C11-O35-C29-C30}(21)+\tau_{C11-O35-C29-O34}(18)$
4	23			0.13	100	$\tau_{C18-C17-C1-O13}(15)+\tau_{C19-C17-C1-C5}(23)+\Gamma_{C19-C17-C1-O13}(16)$
5	33			0.01	6.17	$\tau_{C42-C41-O40-C30}(10)$
6	34			0.13	17.21	$\tau_{CCCC}(3)$
7	38			0.10	22.75	$\tau_{COCC}(30)$
8	39			0.16	20.95	$\tau_{C2-O13-C1-C17}(22)$
9	50			0.04	3.72	$\tau_{C44-O46-C41-O40}(16)$
10	60			0.25	4.79	$\tau_{CCCC}(10)+\tau_{OCCC}(13)$
11	76			0.02	2.30	$\tau_{OCOC}(10)$

12	82		86s	0.37	1.09	τcccc(16)+ Γoccc(13)
13	95			0.09	1.15	$\delta_{C11\text{-}O35\text{-}C29}(10)+ \tau_{C41\text{-}O40\text{-}C30\text{-}C31}(10)$
14	103			0.29	1.01	$\tau_{OCCO}(10)$
15	111			0.62	0.54	$\tau_{OCCC}(13)$
16	114			0.46	0.70	$\tau_{O55C54C32C33}(10)$
17	126			1.04	1.01	$\delta_{C41\text{-}O40\text{-}C30}(12)+ \tau_{C44\text{-}O46\text{-}C41\text{-}O40}(11)$
18	132		140w	0.14	2.02	τccco(10)
19	143			0.34	2.22	$\tau_{OCCC}(10)$
20	169		168w	0.50	1.30	δccc(15)
21	182			0.21	1.36	$\nu_{CC}(10)+\delta_{CCC}(13)+ \tau_{OCCC}(10)$
22	186			2.01	2.70	$\delta_{OCC}(10)$
23	206			3.04	2.61	$\delta_{OCC}(10)$
24	209			0.08	0.99	$\tau_{HCCC}(37)+ \tau_{HCCO}(18)+ \tau_{HCCH}(24)$
25	215			0.36	0.57	$\tau_{C11\text{-}C10\text{-}C8\text{-}O15}(20)$
26	220		220w	1.31	0.59	$\delta_{C45\text{-}C44\text{-}C69}(14) +\tau_{HCCC}(10)$
27	228			1.85	2.90	$\tau_{H56O55C54C32}(10)$
28	229			0.72	0.55	$\tau_{O52C45C44}(10)$
29	240		247w	8.53	3.46	$\tau_{H56\text{-}O55\text{-}C54\text{-}C32}(32)+ \tau_{H56\text{-}O55\text{-}C54\text{-}H57}(22)+ \tau_{H56\text{-}O55\text{-}C54\text{-}H58}(11)$
30	256			0.40	1.88	$\delta_{CCC}(10)$
31	267			0.80	0.96	$\tau_{HOCC}(10)$
32	283			0.36	0.91	$\delta_{CCC}(10)+\delta_{OCC}(10)$
33	284			0.78	1.82	$\tau_{C41O40C30}(10)$
34	293			0.48	0.62	$\tau_{O38C31C30O40}(10)$
35	300			0.94	0.77	$\tau_{OCCC}(10)+ \Gamma_{OCCO}(10)$
36	309			0.43	0.82	$\delta_{O55C54C32}(16)$
37	315			0.10	1.29	$\delta_{OCC}(10)$
38	321			2.60	0.71	$\delta_{OCC}(15)+\delta_{CCO}(10)$
39	340			15.04	2.29	$\tau_{H28\text{-}O27\text{-}C24\text{-}C20}(47)+ \tau_{H28\text{-}O27\text{-}C24\text{-}C22}(52)$
40	345			0.70	0.27	$\delta_{OCC}(14)+\delta_{CCO}(10)+ \tau_{HOCC}(11)$
41	363			2.62	1.00	$\delta_{OCC}(11)+ \tau_{OCCC}(13)$
42	365			12.40	1.06	$\tau_{H53\text{-}O52\text{-}C45\text{-}C43}(29)+ \tau_{H53\text{-}O52\text{-}C45\text{-}C44}(17)+ \tau_{H53\text{-}O52\text{-}C45\text{-}H61}(22)$
43	366			0.69	2.83	$\delta_{OCC}(10)$
44	376		385w	0.98	0.86	$\delta_{OCC}(10)$
45	395			6.04	1.46	$\tau_{H51\text{-}O50\text{-}C43\text{-}C45}(14)$
46	399			4.05	0.83	$\delta_{O27\text{-}C24\text{-}C20}(20)+\delta_{O27\text{-}C24\text{-}C22}(23)$
47	402			2.25	0.27	$\delta_{O27\text{-}C24\text{-}C20}(11)$
48	406			0.19	0.29	$\tau_{C24\text{-}C20\text{-}C18\text{-}C17}(18)+ \tau_{C24\text{-}C22\text{-}C19\text{-}C17}(18)$
49	409			3.30	1.23	$\tau_{H51\text{-}O50\text{-}C43\text{-}C42}(11)+ \tau\Gamma_{H51\text{-}O50\text{-}C43\text{-}H62}(12)$

50	417			4.16	1.81	$\tau_{H51\text{-}O50\text{-}C43\text{-}C42}(15)$
51	419			11.62	1.14	$\tau_{H16\text{-}O15\text{-}C8\text{-}C3}(31)+ \tau_{H16\text{-}O15\text{-}C8\text{-}C10}(32)$
52	432			0.49	1.84	$\tau_{HOCC}(13)$
53	435	434w		5.92	0.45	$\tau_{HCCC}(10)$
54	446		448w	4.02	0.95	$\delta_{CCO}(10)$
55	476		469w	0.41	0.41	$\delta_{CCO}(10)$
56	481	481w		1.63	1.09	$\tau_{CCOC}(11)+ \tau_{HOCC}(12)$
57	497			2.25	0.71	$\delta_{CCC}(11)$
58	503			3.69	1.57	$\tau_{HOCC}(13)$
59	514	511w		0.30	0.99	$\delta_{COC}(14)$
60	517			3.71	0.52	$\delta_{C10C8C3}(10)$
61	523	522w	520w	3.30	3.07	$\nu_{CC}(10)+\nu_{OC}(10)+ \tau_{HOCC}(22)+ \tau_{HOCH}(10)$
62	541			1.15	1.65	$\delta_{CCC}(10)$
63	546			2.37	1.18	$\delta_{CCC}(10)$
64	548		563w	1.26	1.93	$\nu_{CC}(10)$
65	576	561w		0.31	0.67	$\delta_{OCC}(13)$
66	597			2.97	1.77	$\delta_{OCC}(11)$
67	605	608w	607w	2.01	0.48	$\tau_{HCCC}(10)$
68	616			1.10	4.59	$\tau_{CCCC}(10)+ \tau_{CCCH}(10)$
69	621	626w		0.97	0.15	$\tau_{CCCC}(12)+ \tau_{OCCC}(10)$
70	630	637w		1.21	2.15	$\delta_{CCC}(35)$
71	642		643w	0.81	3.90	$\nu_{CC}(16)$
72	661		663ms	0.30	0.67	$\delta_{COC}(12)$
73	666	668w		4.51	0.24	$\tau_{CCOC}(14)$
74	682			0.94	2.08	$\nu_{CC}(21)$
75	700	702w	704w	7.31	0.71	$\tau_{H37\text{-}O36\text{-}C33\text{-}C31}(10)$
76	706			2.47	0.58	$\tau_{CCCC}(26)$
77	713			8.57	0.83	$\tau_{HOCC}(20)$
78	718	730w		0.23	0.55	$\tau_{CCCC}(31)+ \tau_{OCCC}(21)$
79	752	743w	748w	14.50	0.21	$\tau_{H49\text{-}O48\text{-}C42\text{-}C41}(30)+ \tau_{H49\text{-}O48\text{-}C42\text{-}C43}(27)+ \tau_{H49\text{-}O48\text{-}C42\text{-}H63}(14)$
80	774			5.37	0.49	$\tau_{HOCC}(22)+ \tau_{HOCH}(10)$
81	784			2.59	1.96	$\tau_{H12\text{-}C10\text{-}C8\text{-}O15}(20)+ \tau_{O35\text{-}C11\text{-}C10\text{-}H12}(20)$
82	788			2.02	1.41	$\tau_{H25\text{-}C20\text{-}C18\text{-}C17}(20)+ \tau_{C22\text{-}C24\text{-}C20\text{-}H25}(14)+ \tau_{O27\text{-}C24\text{-}C20\text{-}H25}(23)$
83	794			4.26	2.11	$\nu_{C69\text{-}C44}(15)$
84	796			2.84	2.84	$\nu_{O27\text{-}C24}(14)$
85	805			1.86	1.69	$\nu_{CC}(18)+\nu_{OC}(11)$
86	812		812w	6.63	0.48	$\tau_{C24\text{-}C22\text{-}C19\text{-}H23}(13)+ \tau_{H26\text{-}C22\text{-}C19\text{-}C17}(17)+ \tau_{O27\text{-}C24\text{-}C22\text{-}H26}(21)$
87	814			1.23	4.67	$\nu_{O34\text{-}C32}(18)$

88	823	821ms		5.97	0.24	$\nu_{CC}(17)+\nu_{OC}(11)$
89	848	835w	837w	1.61	2.71	$\nu_{C18-C17}(11)$
90	856			0.95	0.28	$\nu_{C33-C31}(14)$
91	871	864vw	864w	0.45	1.47	$\nu_{C43-C42}(15)$
92	876	888w		2.61	0.89	$\nu_{O13-C1}(16)$
93	877			6.17	0.34	$\nu_{CC}(22)+\nu_{OC}(23)$
94	910		896ms	0.22	0.34	$\tau_{H21-C18-C17-C1}(15)+\tau_{C24-C20-C18-H21}(11)+\tau_{H25-C20-C18-H21}(35)$
95	922	919w		0.01	0.12	$\tau_{H23-C19-C17-C1}(12)+\tau_{H23-C19-C17-C18}(11)+\tau_{H26-C22-C19-H23}(36)$
96	923			1.76	2.11	$\nu_{O46-C44}(17)+\delta_{H-C-C}(13)$
97	953			0.54	0.74	$\nu_{O13-C1}(11)+\tau_{HCCC}(10)$
98	961			1.34	1.10	$\nu_{C45-C43}(24)+\delta_{H72-C69-C44}(11)+\tau_{H70-C69-C44}(10)$
99	963			2.63	0.87	$\nu_{C31-C30}(13)+\nu_{O36-C33}(12)$
100	987	986ms	982w	28.45	4.40	$\nu_{O35-C29}(20)$
101	990		1002w	3.25	0.12	$\nu_{CC}(31)+\delta_{CCC}(32)+\delta_{CCH}(18)+\delta_{HCC}(14)$
102	1004			10.29	1.40	$\nu_{O38-C}31(11)$
103	1011			38.88	0.64	$\nu_{OC}(16)+\nu_{CC}(12)$
104	1021			8.50	1.82	$\nu_{OC}(16)+\nu_{CC}(10)$
105	1025			8.95	0.44	$\nu_{CC}(11)+\nu_{CO}(32)+\nu_{C69-C44}(10)$
106	1032			13.48	0.82	$\nu_{C33-C32}(14)$
107	1038			15.47	0.66	$\nu_{O40-C30}(11)+\nu_{O55-C54}(24)$
108	1039		1039w	15.09	0.88	$\nu_{C5-C1}(14)+\nu_{C33-C32}(14)$
109	1040	1040s		3.50	3.12	$\nu_{C5-C1}(19)+\nu_{O13-C1}(11)$
110	1053			57.67	0.97	$\nu_{C41-O40}(20)+\nu_{O46-C41}(18)+\nu_{O52-C45}(18)$
111	1063	1060s		33.94	1.22	$\nu_{O13-C2}(12)+\nu_{O15-C8}(11)+\nu_{O55-C54}(19)$
112	1066			2.32	1.28	$\nu_{O55-C54}(16)+\nu_{CO}(35)$
113	1070			6.68	0.27	$\nu_{CO}(42)$
114	1073			7.73	0.99	$\nu_{CO}(26)$
115	1076	1071s		7.75	0.30	$\nu_{O36-C33}(19)$
116	1082		1081ms	25.65	1.70	$\nu_{O38-C31}(15)+\nu_{C41-O40}(11)+\nu_{O48-C42}(11)$
117	1087	1089s		1.36	0.95	$\nu_{C22-C19}(15)+\delta_{H26-C22-C19}(14)$
118	1095			15.05	0.57	$\nu_{CO}(18)$
119	1100			12.86	1.28	$\nu_{O48-C42}(29)+\nu_{O52-C45}(24)$
120	1104			15.31	1.13	$\nu_{C54-C32}(11)$
121	1107			12.96	0.88	$\nu_{O50-C43}(12)+\nu_{O52-C45}(13)$
122	1116		1122ms	8.29	0.35	$\delta_{H53-O52-C45}(11)+\Gamma_{HCCH}(10)$
123	1134	1136s		17.14	0.89	$\nu_{O46-C41}(15)+\delta_{CCH}(10)$
124	1142			3.17	2.44	$\nu_{CO}(19)+\delta_{CCH}(14)$
125	1152			14.20	1.00	$\delta_{H21-C18-C17}(10)+\delta_{H26-C22-C19}(11)+\delta_{C24-C22-H26}(12)$

126	1153			2.97	0.92	$\delta_{C24\text{-}C20\text{-}H25}(10)+\delta_{H28\text{-}O27\text{-}C24}(35)$
127	1159			41.82	1.39	$\delta_{HCC}(14)+\nu_{C\text{-}O}(23)$
128	1175	1178s		2.39	0.59	$\nu_{C10\text{-}C8}(11)+\delta_{H12\text{-}C10\text{-}C8}(13)+\delta_{H16\text{-}O15\text{-}C8}(36)$
129	1180		1185w	3.80	1.01	$\delta_{H56\text{-}O55\text{-}C54}(24)+\delta_{CCH}(10)+\delta_{H37\text{-}O36\text{-}C33}(10)$
130	1189			16.87	1.40	$\nu_{C17C1}(11)$
131	1191			1.29	4.38	$\nu_{C17\text{-}C1}(18)$
132	1201			5.32	0.05	$\delta_{H51\text{-}O50\text{-}C43}(17)$
133	1203	1205s	1210s	12.61	4.78	$\nu_{C4\text{-}C3}(10)$
134	1217		1215w	3.99	0.92	$\delta_{H56\text{-}O55\text{-}C54}(23)+\delta_{H58\text{-}C54\text{-}C32}(12)+\delta_{O55\text{-}C54\text{-}H58}(10)$
135	1224			2.95	1.24	$\delta_{H53\text{-}O52\text{-}C45}(31)$
136	1227			1.00	0.77	$\delta_{H68\text{-}C5\text{-}C1}(16)+\delta_{H68\text{-}C5\text{-}C4}(15)$
137	1245			0.96	0.93	$\delta_{H57\text{-}C54\text{-}C32}(13)$
138	1248			7.72	0.73	$\delta_{H49\text{-}O48\text{-}C42}(14)$
139	1254		1254w	41.32	6.38	$\nu_{C4\text{-}C3}(18)+\delta_{H16\text{-}O15\text{-}C8}(19)$
140	1256			1.73	0.24	$\delta_{C43\text{-}C42\text{-}H63}(11)$
141	1259			8.28	2.64	$\nu_{O27\text{-}C24}(48)$
142	1260	1263w		0.21	0.44	$\delta_{HOC}(14)$
143	1279			0.17	1.21	$\delta_{CCH}(22)$
144	1284	1282w		5.76	0.62	$\nu_{C18\text{-}C17}(12)$
145	1297	1296s		1.93	1.15	$\nu_{C45\text{-}C44}(11)+\delta_{O46\text{-}C44\text{-}H60}(11)$
146	1310			6.20	1.91	$\delta_{CCH}(14)+\delta_{OCH}(10)$
147	1312			6.75	1.57	$\delta_{CCH}(13)+\delta_{OCH}(10)+\nu_{COCH}(12)$
148	1315			5.24	0.39	$\delta_{H51\text{-}O50\text{-}C43}(23)$
149	1322			11.27	0.37	$\nu_{CC}(15)$
150	1324			0.67	1.01	$\delta_{H28\text{-}O27\text{-}C24}(10)$
151	1328			5.73	0.68	$\nu_{CC}(31)$
152	1331			2.80	0.65	$\delta_{CCH}(10)$
153	1334			4.28	0.43	$\delta_{HOC}(10)+\Gamma_{HCCH}(11)$
154	1338			0.28	0.41	$\delta_{O34\text{-}C32\text{-}H66}(12)$
155	1344	1341ms		7.17	1.37	$\delta_{OCC}(10)$
156	1345			1.95	0.85	$\delta_{HCC}(25)$
157	1349		1348ms	1.73	0.32	$\delta_{HCC}(13)+\Gamma_{HCCH}(11)$
158	1354			11.74	1.66	$\nu_{O15\text{-}C8}(12)$
159	1357			3.85	0.21	$\delta_{HOC}(11)$
160	1363	1363ms		1.88	0.30	$\delta_{H71\text{-}C69\text{-}H72}(20)+\delta_{HCC}(18)$
161	1370		1373w	0.57	0.51	$\delta_{O34\text{-}C29\text{-}H67}(12)+\Gamma_{H59\text{-}C30\text{-}C29\text{-}H67}(11)$
162	1378			1.81	0.62	$\delta_{HOC}(12)+\delta_{HCO}(10)$
163	1383			2.41	0.34	$\delta_{COH}(11)$
164	1390	1393ms		12.51	0.24	$\delta_{H39\text{-}O38\text{-}C31}(33)$

165	1399			2.48	0.80	$\delta_{H37\text{-}O36\text{-}C33}(26)+\delta_{H49\text{-}O48\text{-}C42}(14)$
166	1407			1.85	0.15	$\delta_{H51\text{-}O50\text{-}C43}(13)+\delta_{HOC}(18)$
167	1408			1.25	1.84	$\delta_{H9\text{-}C5\text{-}H68}(31)+\Gamma_{HCCC}(25)+\Gamma_{HCCO}(25)+\Gamma_{HCCH}(10)$
168	1411			10.03	1.15	$\delta_{H37\text{-}O36\text{-}C33}(15)+\delta_{H39\text{-}O38\text{-}C31}(14)+\delta_{H49\text{-}O48\text{-}C42}(17)$
169	1420			13.63	0.06	$\nu_{CC}(29)+\delta_{CCH}(11)$
170	1423			1.69	0.28	$\delta_{H56\text{-}O55\text{-}C54}(13)+\delta_{H57\text{-}C54\text{-}C32}(25)+\Gamma_{HOCC}(19)$
171	1429			16.16	0.06	$\delta_{CCC}(25)+\delta_{CCH}(11)$
172	1447			0.60	1.85	$\delta_{H70\text{-}C69\text{-}C44}(11)+\delta_{H70\text{-}C69\text{-}H71}(24)+\delta_{H71\text{-}C69\text{-}H72}(23)$
173	1450	1453ms	1456ms	0.08	1.04	$\delta_{H70\text{-}C69\text{-}H72}(39)+\Gamma_{HCCH}(10)$
174	1466			0.99	1.30	$\delta_{H57\text{-}C54\text{-}H58}(30)+\Gamma_{HCCC}(16)+\Gamma_{HCCO}(16)+\Gamma_{HCCH}(17)$
175	1473			4.50	0.18	$\nu_{C11\text{-}C7}(17)$
176	1502	1502ms	1502vw	12.45	0.71	$\nu_{C18\text{-}C17}(10)$
177	1561		1574ms	20.70	0.96	$\nu_{C3\text{-}C2}(12)+\nu_{C8\text{-}C3}(13)+\nu_{C11\text{-}C7}(12)+\nu_{C11\text{-}C10}(28)$
178	1584	1582ms		3.29	0.61	$\nu_{C18\text{-}C17}(11)+\nu_{C19\text{-}C17}(20)+\nu_{C24\text{-}C20}(20)+\nu_{C24\text{-}C22}(17)$
179	1598			105.6	14.03	$\nu_{C7\text{-}C2}(22)+\nu_{C10\text{-}C8}(20)+\nu_{C11\text{-}C7}(12)$
180	1610			7.51	8.61	$\nu_{C20\text{-}C18}(20)+\nu_{C22\text{-}C19}(20)+\nu_{C24\text{-}C22}(10)$
181	1710	1646s	1643vs	36.22	7.18	$\nu_{O14\text{-}C4}(87)$
182	2865			6.63	2.26	$\nu_{C54\text{-}H57}(70)+\nu_{C54\text{-}H58}(30)$
183	2873			0.65	0.73	$\nu_{C41\text{-}H47}(20)+\nu_{C45\text{-}H61}(33)+\nu_{C43\text{-}H62}(39)$
184	2883			2.33	1.37	$\nu_{C41\text{-}H47}(39)+\nu_{C45\text{-}H61}(11)+\nu_{C43\text{-}H62}(49)$
185	2888	2890w		3.24	1.62	$\nu_{C1\text{-}H73}(97)$
186	2890			4.81	2.82	$\nu_{C41\text{-}H47}(29)+\nu_{C45\text{-}H61}(51)+\nu_{C42\text{-}H63}(19)$
187	2904		2899ms	4.31	1.64	$\nu_{C54\text{-}H57}(28)+\nu_{C54\text{-}H58}(69)$
188	2907			13.46	0.29	$\nu_{C41\text{-}H47}(12)+\nu_{C43\text{-}H62}(12)+\nu_{C42\text{-}H63}(70)$
189	2927	2929w		1.27	1.28	$\nu_{C5\text{-}H9}(87)+\nu_{C5\text{-}H68}(11)$
190	2938			1.52	3.52	$\nu_{C44\text{-}H60}(13)+\nu_{C69\text{-}H70}(41)+\nu_{C69\text{-}H71}(20)+\nu_{C69\text{-}H72}(25)$
191	2939		2939w	2.77	0.78	$\nu_{C29\text{-}H67}(97)$
192	2941			4.72	1.18	$\nu_{C44\text{-}H60}(83)$
193	2943			1.93	1.77	$\nu_{C33\text{-}H65}(23)+\nu_{C32\text{-}H66}(73)$
194	2952		2958w	1.95	0.98	$\nu_{C31\text{-}H64}(23)+\nu_{C33\text{-}H65}(55)+\nu_{C32\text{-}H66}(21)$
195	2965			6.01	2.23	$\nu_{C31\text{-}H64}(73)+\nu_{C33\text{-}H65}(22)$
196	2985	2970w	2976w	2.17	1.36	$\nu_{C30\text{-}H59}(95)$
197	3005			1.16	2.05	$\nu_{C5\text{-}H9}(10)+\nu_{C5\text{-}H68}(89)$
198	3008			4.42	0.75	$\nu_{C69\ H70}(52)+\nu_{C69\text{-}H72}(42)$
199	3021			1.75	1.53	$\nu_{C69\text{-}H71}(71)+\nu_{C69\text{-}H72}(25)$
200	3042			3.33	1.72	$\nu_{C20\text{-}H25}(96)$
201	3053			1.14	1.28	$\nu_{C19\text{-}H23}(95)$
202	3083		3071w	0.88	0.96	$\nu_{C18\text{-}H21}(95)$

203	3089			0.86	3.57	$\nu_{C22-H26}$(94)
204	3096			0.89	1.70	$\nu_{C10-H12}$(100)
205	3114			0.01	1.24	ν_{C7-H6}(100)
206	3425	3427s		69.82	1.75	$\nu_{O48-H49}$(95)
207	3497			12.72	0.40	$\nu_{O38-H39}$(92)
208	3555			17.68	0.40	$\nu_{O36-H37}$(97)
209	3603			8.26	0.53	$\nu_{O50-H51}$(100)
210	3653			5.73	1.47	$\nu_{O15-H16}$(100)
211	3658			4.70	1.07	$\nu_{O52-H53}$(100)
212	3672			7.22	1.56	$\nu_{O27-H28}$(100)
213	3680			3.36	1.75	$\nu_{O55-H56}$(100)

[v]: Stretching, δ: In-plane-bending, γ: Out-of-plane bending, vw: Very week, w: Week, m: Medium, s: Strong, vs: Very strong, Scaling factor: 0.9608 (palafox, 2000),
[b] Relative IR Absorption intensities normalized with highest peak absorption equal to 100,
[c] Relative raman intensities calculated by equation (2.1) and normalized to 100.
[d] Total energy distribution calculated at B3LYP/6-31G(d,p) level.

harmonic bands 961, 1116 cm^{-1} (mode numbers: 98, 122) are assigned as rocking modes of CH_3. The torsion vibrations are not observed in the FT-IR spectrum because this appears at very low frequency. The FT-Raman experimental band observed at 220 cm^{-1} shows an excellent agreement with theoretical results. These assignments support from the work of Sundaraganesan et al. and are within the frequency intervals given by Varsanyi [25, 26].

Methylene Group (CH_2) Vibrations

In present molecule, two methylene groups are available, which are attached in Naringenin core and in D-glucose structure. In which, the methylene group in Naringenin core has observed at higher frequency than in ring D. The symmetric and asymmetric (H_{68}-C_5-H_9) stretching modes are assigned to 2929 cm^{-1}/FT-IR (2927/mode number: 189) and 3005 cm^{-1} (mode number: 197) respectively. Similarly, the harmonic bands 2865 cm^{-1} (mode number: 182) and 2904 (mode number: 187)/ 2899 cm^{-1}: Raman are assigned to δCH_2 (sym) and δCH_2 (H_{57}-C_{54}-H_{58}) (asym) mode respectively. These assignments are well comparable and also find support from TED column. The methylene group has six normal modes of vibrations, namely CH_2 symmetric (νsym), CH_2 asymmetric (νasym), scissoring (δ), rocking (ρ), wagging (ω) and twisting (t) modes are able to appear in the range 1500-800 cm^{-1} [22].

In this molecule, there are two CH_2 groups (ring B & D). The general order of CH_2 deformation is: CH_2 scissoring > CH_2 wagging > CH_2 twisting > CH_2 rocking. In the present study, the CH_2 bending modes follow the same trend. Since the bending modes involving hydrogen atom attached to the central carbon fall into the range 1450-875 cm^{-1} there are extensive vibrational coupling of these modes with CH_2 deformations particularly with the CH_2 twist [26]. It is notable that both CH_2 scissoring and CH_2 rocking were sensitive to the molecular conformation. The mode numbers: 167, 174 are belonging to the δCH_2 mode. The frequencies observed at 1185 cm^{-1} (FT-Raman) and at 1136 cm^{-1} (FT-IR) are assigned to CH_2 wagging and CH_2 twisting, respectively. The other fundamental mode of CH_2 (rocking: mode number: 97) is observed in the expected region and also presented in Table 1. These assignments are found to be satisfactorily in agreement with the reported values [27].

O-H Vibrations

The broad, intense –OH stretching absorption from 3300 to 2500 cm^{-1} suggests the presence of carboxylic group in the Naringin extracted from kinnow peel. The strong and broad hydrogen bonded O-H stretching bands centering 3300 and 3400 cm^{-1} are for alcohols and phenols, respectively [28]. The hydroxyl group vibrations are appeared in the higher range than other vibrations. In our study, the O-H group stretching vibration of A, B, C, D and E rings are lies at different frequencies. In this molecule, the mode numbers: 213, 208, 207 and 211, 209, 206 are assigned to the ν(OH) for ring D and ring E, respectively. The harmonic values 3653 cm^{-1} (mode number: 210/ring A) and 3672 cm^{-1} (mode number: 212/ring C) are belong to the core molecule of Naringin. The experimental νOH group vibration has observed at 3427 cm^{-1} as a shoulder band in FT-IR spectrum, which is exactly matches with the literature value 3433 cm^{-1} [29].

The OH in-plane bending vibration appears in the range of 1440-1395 cm^{-1}. Akkaya and Akyüz et al. assigned this vibration at 1294 and 1160 cm^{-1} in IR for 4-aminosalicylic acid [18, 30]. For 3-aminosalicylic acid, this band is observed at 1340 and 1171 cm^{-1} which is a motion of hydroxyl group [31]. In the present work, the O-H in-plane bending mode is assigned to 1393 cm^{-1} in FT-IR and 1254, 1185, 1122 cm^{-1} in FT-Raman experimentally, which are calculated at 1390, 1254, 1180, 1116 (mode numbers: 164, 139, 129, 122) for Naringin. The above assignments are supported by TED values. The δCOH and τCOH vibrations (harmonic) are calculated in the regions 1423-1153 cm^{-1} (mode numbers: 170-126) and 774-228 cm^{-1} (mode numbers: 80-27), respectively. The observed bands 1215 (FT-Raman), 1263 cm^{-1}(FT-IR) and

Table 1: The vibrational assignments of Naringin using Scaled Quantum Mechanics method (B3LYP/6-31G(d,p)).

Scaled B3LYP[a]	FT-IR	FT-Raman	I^b_{IR}	I^c_{Raman}	Vibrational assignments TED[d] (≥ 10)
82		86s	0.37	1.09	τcccc(16)+ Γoccc(13)
132		140w	0.14	2.02	τccco(10)
169		168w	0.50	1.30	δccc(15)
220		220w	1.31	0.59	$\delta_{C45\text{-}C44\text{-}C69}(14) + \tau_{HCCC}(10)$
240		247w	8.53	3.46	$\tau_{H56\text{-}O55\text{-}C54\text{-}C32}(32) + \tau_{H56\text{-}O55\text{-}C54\text{-}H57}(22) + \tau_{H56\text{-}O55\text{-}C54\text{-}H58}(11)$
376		385w	0.98	0.86	$\delta_{OCC}(10)$
435	434w		5.92	0.45	$\tau_{HCCC}(10)$
446		448w	4.02	0.95	$\delta_{CCO}(10)$
476		469w	0.41	0.41	$\delta_{CCO}(10)$
481	481w		1.63	1.09	$\tau_{CCOC}(11) + \tau_{HOCC}(12)$
514	511w		0.30	0.99	$\delta_{COC}(14)$
523	522w	520w	3.30	3.07	$\nu_{CC}(10) + \nu_{OC}(10) + \tau_{HOCC}(22) + \tau_{HOCH}(10)$
548		563w	1.26	1.93	$\nu_{CC}(10)$
576	561w		0.31	0.67	$\delta_{OCC}(13)$
597			2.97	1.77	$\delta_{OCC}(11)$
605	608w	607w	2.01	0.48	$\tau_{HCCC}(10)$
616			1.10	4.59	$\tau_{CCCC}(10) + \tau_{CCCH}(10)$
621	626w		0.97	0.15	$\tau_{CCCC}(12) + \tau_{OCCC}(10)$
630	637w		1.21	2.15	$\delta_{CCC}(35)$
642		643w	0.81	3.90	$\nu_{CC}(16)$
661		663ms	0.30	0.67	$\delta_{COC}(12)$
666	668w		4.51	0.24	$\tau_{CCOC}(14)$
700	702w	704w	7.31	0.71	$\tau_{H37\text{-}O36\text{-}C33\text{-}C31}(10)$
718	730w		0.23	0.55	$\tau_{CCCC}(31) + \tau_{OCCC}(21)$
752	743w	748w	14.50	0.21	$\tau_{H49\text{-}O48\text{-}C42\text{-}C41}(30) + \tau_{H49\text{-}O48\text{-}C42\text{-}C43}(27) + \tau_{H49\text{-}O48\text{-}C42\text{-}H63}(14)$
812		812w	6.63	0.48	$\tau_{C24\text{-}C22\text{-}C19\text{-}H23}(13) + \tau_{H26\text{-}C22\text{-}C19\text{-}C17}(17) + \tau_{O27\text{-}C24\text{-}C22\text{-}H26}(21)$
823	821ms		5.97	0.24	$\nu_{CC}(17) + \nu_{OC}(11)$
848	835w	837w	1.61	2.71	$\nu_{C18\text{-}C17}(11)$
871	864vw	864w	0.45	1.47	$\nu_{C43\text{-}C42}(15)$
876	888w		2.61	0.89	$\nu_{O13\text{-}C1}(16)$
910		896ms	0.22	0.34	$\tau_{H21\text{-}C18\text{-}C17\text{-}C1}(15) + \tau_{C24\text{-}C20\text{-}C18\text{-}H21}(11) + \tau_{H25\text{-}C20\text{-}C18\text{-}H21}(35)$
922	919w		0.01	0.12	$\tau_{H23\text{-}C19\text{-}C17\text{-}C1}(12) + \tau_{H23\text{-}C19\text{-}C17\text{-}C18}(11) + \tau_{H26\text{-}C22\text{-}C19\text{-}H23}(36)$
987	986ms	982w	28.45	4.40	$\nu_{O35\text{-}C29}(20)$
990		1002w	3.25	0.12	$\nu_{CC}(31) + \delta_{CCC}(32) + \delta_{CCH}(18) + \delta_{HCC}(14)$
1039		1039w	15.09	0.88	$\nu_{C5\text{-}C1}(14) + \nu_{C33\text{-}C32}(14)$

1040	1040s		3.50	3.12	$\nu_{C5\text{-}C1}(19)+\nu_{O13\text{-}C1}(11)$
1063	1060s		33.94	1.22	$\nu_{O13\text{-}C2}(12)+\nu_{O15\text{-}C8}(11)+\nu_{O55\text{-}C54}(19)$
1076	1071s		7.75	0.30	$\nu_{O36\text{-}C33}(19)$
1082		1081ms	25.65	1.70	$\nu_{O38\text{-}C31}(15)+\nu_{C41\text{-}O40}(11)+\nu_{O48\text{-}C42}(11)$
1087	1089s		1.36	0.95	$\nu_{C22\text{-}C19}(15)+\delta_{H26\text{-}C22\text{-}C19}(14)$
1116		1122ms	8.29	0.35	$\delta_{H53\text{-}O52\text{-}C45}(11)+\Gamma_{HCCH}(10)$
1134	1136s		17.14	0.89	$\nu_{O46\text{-}C41}(15)+\delta_{CCH}(10)$
1175	1178s		2.39	0.59	$\nu_{C10\text{-}C8}(11)+\delta_{H12\text{-}C10\text{-}C8}(13)+\delta_{H16\text{-}O15\text{-}C8}(36)$
1180		1185w	3.80	1.01	$\delta_{H56\text{-}O55\text{-}C54}(24)+\delta_{CCH}(10)+\delta_{H37\text{-}O36\text{-}C33}(10)$
1203	1205s	1210s	12.61	4.78	$\nu_{C4\text{-}C3}(10)$
1217		1215w	3.99	0.92	$\delta_{H56\text{-}O55\text{-}C54}(23)+\delta_{H58\text{-}C54\text{-}C32}(12)+\delta_{O55\text{-}C54\text{-}H58}(10)$
1254		1254w	41.32	6.38	$\nu_{C4\text{-}C3}(18)+\delta_{H16\text{-}O15\text{-}C8}(19)$
1260	1263w		0.21	0.44	$\delta_{HOC}(14)$
1284	1282w		5.76	0.62	$\nu_{C18\text{-}C17}(12)$
1297	1296s		1.93	1.15	$\nu_{C45\text{-}C44}(11)+\delta_{O46\text{-}C44\text{-}H60}(11)$
1344	1341ms		7.17	1.37	$\delta_{OCC}(10)$
1349		1348ms	1.73	0.32	$\delta_{HCC}(13)+\Gamma_{HCCH}(11)$
1363	1363ms		1.88	0.30	$\delta_{H71\text{-}C69\text{-}H72}(20)+\delta_{HCC}(18)$
1370		1373w	0.57	0.51	$\delta_{O34\text{-}C29\text{-}H67}(12)+\Gamma_{H59\text{-}C30\text{-}C29\text{-}H67}(11)$
1390	1393ms		12.51	0.24	$\delta_{H39\text{-}O38\text{-}C31}(33)$
1450	1453ms	1456ms	0.08	1.04	$\delta_{H70\text{-}C69\text{-}H72}(39)+\Gamma_{HCCH}(10)$
1502	1502ms	1502vw	12.45	0.71	$\nu_{C18\text{-}C17}(10)$
1561		1574ms	20.70	0.96	$\nu_{C3\text{-}C2}(12)+\nu_{C8\text{-}C3}(13)+\nu_{C11\text{-}C7}(12)+\nu_{C11\text{-}C10}(28)$
1584	1582ms		3.29	0.61	$\nu_{C18\text{-}C17}(11)+\nu_{C19\text{-}C17}(20)+\nu_{C24\text{-}C20}(20)+\nu_{C24\text{-}C22}(17)$
1710	1646s	1643vs	36.22	7.18	$\nu_{O14\text{-}C4}(87)$
2888	2890w		3.24	1.62	$\nu_{C1\text{-}H73}(97)$
2904		2899ms	4.31	1.64	$\nu_{C54\text{-}H57}(28)+\nu_{C54\text{-}H58}(69)$
2927	2929w		1.27	1.28	$\nu_{C5\text{-}H9}(87)+\nu_{C5\text{-}H68}(11)$
2939		2939w	2.77	0.78	$\nu_{C29\text{-}H67}(97)$
2952		2958w	1.95	0.98	$\nu_{C31\text{-}H64}(23)+\nu_{C33\text{-}H65}(55)+\nu_{C32\text{-}H66}(21)$
2985	2970w	2976w	2.17	1.36	$\nu_{C30\text{-}H59}(95)$
3083		3071w	0.88	0.96	$\nu_{C18\text{-}H21}(95)$
3425	3427s		69.82	1.75	$\nu_{O48\text{-}H49}(95)$

[v]: Stretching, δ: In-plane-bending, τ: Out-of-plane bending, vw: very weak, m: medium, s: Strong, vs: very strong,
[a]Scaled computed wavenumber using scale factor: 0.9608 (palafox, 2000),
[b] Relative IR Absorption intensities normalized with highest peak absorption equal to 100,
[c] Relative raman intensities calculated by equation (2.1) and normalized to 100.
[d] Total energy distribution calculated at B3LYP/6-31G(d,p) level.

743/748 cm^{-1} (FT-IR/FT-Raman), 247 cm^{-1}: FT-Raman supports the above assignments.

C=O and C-O Vibrations

Normal esters are characterized by strong IR absorption due to the carbonyl (C=O) stretching vibration in the range 1750-1735 cm^{-1} [32]. The FT-IR and FT-Raman spectra show the vibrational frequency for C=O at 1646 cm^{-1} and 1633 cm^{-1} respectively [33, 29]. The presence of carbonyl group on Naringin can be confirmed from peak situated at 1634 cm^{-1} [34]. The carbonyl stretching vibration observed as an intense band at 1603 cm^{-1} for 6-aminoflavone in FT-IR. The observed wavenumber of the carbonyl stretching vibration is lower due to π-electron being localized [22]. In the present study the C_4=O_{14} stretching vibrations is appeared at 1646 (strong) and 1643 cm^{-1} (very strong) band in FT-IR and FT-Raman spectra respectively, while the harmonic value is 1710 cm^{-1} (mode number: 181).

In 2, 6-dichloro-4-nitrophenol, the $\nu_{C\text{-}O}$ vibrations lie in the region 1095-1310 cm^{-1} [35]. In our study, the $\nu_{C\text{-}O}$ vibrations are observed at different frequencies in different rings (A, B, C, D & E). The computed wavenumbers in the range 1354-1053 cm^{-1} (mode numbers: 158, 141, 124, 123, 121, 119, 118, 116-110) are assigned to $\nu_{C\text{-}O}$ mode. These vibrations have considerable TED and also find support from 1136, 1071, 1060 cm^{-1} (FT-IR) and 1081 cm^{-1} (FT-Raman). In ring B, the νO_{13}-C_2 is observed at higher frequency (1060 cm^{-1}: FT-IR/1063: mode number: 111) than the νO_{13}-C_1 (1040 cm^{-1}: FT-IR/1040: mode number: 109). The harmonic values C_{41}-O_{46}:1053 cm^{-1}/mode number: 110 and C_{32}-O_{34}:814 cm^{-1}/mode number: 87 are belongs to ring E and ring D, respectively.

Similarly the computed values 1066 cm^{-1}/mode number: 112, 1038 cm^{-1}/mode number: 107 and 987 cm^{-1}/mode number: 100 are belongs to C_{54}-O_{55}, C_{30}-O_{40} and C_{29}-O_{35} stretching vibrations, respectively.

C-C Vibrations

The ring C-C stretching occurs in the region 1625-1430 cm^{-1}. The six member aromatic ring has two or three strong bands in the region about 1500 cm^{-1} are being due to skeletal vibration [33]. The C-C stretching bands for aromatic ring usually appear between 1600 and 1450 cm^{-1}. The C-C stretching of alkenes appeared at 1650 cm^{-1} [36, 29]. In the present study, the FT-IR bands at 1582, 1502 (in ring C), and FT-Raman bands at 1574 (ring A), 1502 cm^{-1} (in ring C) are assigned to $\nu_{C\text{-}C}$ mode. The calculated $\nu_{C\text{-}C}$ frequencies are in the range 1610-1473 cm^{-1} using B3LYP/6-31G (d, p) level. In which the mode numbers: 179, 177, 175 and 180, 178, 176 are belongs to ring A and ring C, respectively. The harmonic vibrations 1297 (ring E), 1284 (ring C), 1254 (ring B), 1203 (ring B), 1175 (ring A), 1087 (ring C), 1040 (ring B), 1039 (ring D), 1032 cm^{-1} (ring D) are also attributed to $\nu_{C\text{-}C}$ mode. These assignments are supported by 1296, 1282, 1205, 1178, 1089, 1040 cm^{-1} (FT-IR) and 1254, 1210 1039 cm^{-1} (FT-Raman) observed bands and also have considerable TED values. The $\nu_{C\text{-}C}$ vibrations (other than ring) 1191 cm^{-1}/mode no: 131, 1104 cm^{-1}/ mode no: 120 and 1025 cm^{-1}/mode no: 105 are belongs to C_{17}-C_1, C_{54}-C_{32} and C_{69}-C_{44}, respectively.

In-plane bending deformation δ_{HCC} and δ_{CCH} are observed at 1348 (FT-Raman), 1215 (FT-Raman), 1178 (FT-IR), 1089 (FT-IR) and 1002 cm^{-1} (FT-Raman) respectively. The observed FT-IR bands: 919, 608, 434 cm^{-1}/Raman: 896, 812, 607 cm^{-1} and FT-Raman bands: 896, 812 cm^{-1} are assigned to τ_{HCC} and τ_{CCH} modes, respectively. Erdoğdu et al., observed the δ_{CCH} mode in the region 1495-1001 cm^{-1} and τ_{CCH} mode in the region (FT-IR) 923-451 cm^{-1} for 6,8-dichloroflavone [33]. The ring breathing mode was calculated at 990 cm^{-1}/ mode number: 101 for Naringin and was observed at 1002 cm^{-1} in Raman spectra. These assignments are in line with literature [33].

NBO Analysis

The hyperconjugation may be given as stabilizing effect that arises from an overlap between an occupied orbital with another neighboring electron deficient orbital, when these orbitals are properly orientated. This non-covalent bonding-antibonding interaction can be quantitatively described in terms of the NBO analysis, which is expressed by means of the second-order perturbation interaction energy (E(2)) [37-40][46-49]. This energy represents the estimate of the off-diagonal NBO Fock matrix elements. It can be deduced from the second-order perturbation approach [41]

$$E^2 = \Delta E_{ij} = q_i \frac{F(i,j)^2}{\varepsilon_j - \varepsilon_i} \qquad (2)$$

where q_i is the donor orbital occupancy, ε_i and ε_j are diagonal elements (orbital energies) and F (i, j) is the off diagonal NBO Fock matrix elements.

The NBO analysis has been carried out to elucidate the intra-molecular interaction among natural bond orbitals, the results of NBO analysis are presented in Table 2. In the present investigation, the π- π* interaction are mainly interested. Here the electron densities of conjugated π bonds are lower than the σ bond. Whereas, the delocalization is more while the transition from π bond to π* bond. The larger $E^{(2)}$ value, denotes that the more delocalization takes place into a particular bond, it mainly occurs during π-π* transition. Moreover, as mentioned above the electron densities in donor (i) π bonds decreases, at the same time electron density increases in acceptor (j) π* bonds. It is evident from the Table 2 the donor (π) bonds have 1.678, 1.621, 1.667, 1.702 and 1.652e as electron densities for C_2-C_7, C_3-C_8, C_{17}-C_{18}, C_{19}-C_{22} & C_{20}-C_{24} bond, respectively. These electron densities are relatively lesser than the σ bonds. On the other hand, the strong delocalization occurs between donor (π: C_2-C_7, C_3-C_8, C_{17}-C_{18}, C_{19}-C_{22} and C_{20}-C_{24} bonds) and acceptor (π*: C_3-C_8, C_2-C_7, C_{19}-C_{22}, C_{17}-C_{18} and C_{17}-C_{18} bonds) bonds, and the electron densities relatively increased in acceptor bonds and hence leading to more stabilization energies are obtained as 51.46, 126.44, 96.23, 75.02 and 94.73 kJ/mol, respectively. The NBO analysis explores the insights of intra molecular interactions among the intra bonds in Naringin molecule.

Table 2: Second order perturbation theory analysis of Fock matrix in NBO basis for Naringin using B3LYP/6-31G(d,p) basis set.

Type	Donor (i)	ED/e	Acceptor (j)	ED/e	$E^{(2)}$ kJ/mol [a]
π-π*	C_2-C_7(2)	1.678	C_3-C_8(2)	0.468	51.46
			C_{10} –C_{11}(2)	0.429	121.92
π-π*	C_3-C_8(2)	1.621	C_2-C_7(2)	0.387	126.44
			C_4-O_{14}(2)	0.159	92.05
			C_{10}-C_{11}(2)	0.429	54.56
π-π*	C_{10} – C_{11}(2)	1.973	C_2-C_7(2)	0.387	52.51
			C_3-C_8(2)	0.468	122.47
π-π*	C_{17}-C_{18}(2)	1.667	C_{19}-C_{22}(2)	0.335	96.23
			C_{20}-C_{24}(2)	0.394	75.56
π-π*	C_{19}-C_{22}(2)	1.702	C_{17}-C_{18}(2)	0.361	75.02
			C_{20}-C $_{24}$(2)	0.394	95.60
π-π*	C_{20}-C_{24}(2)	1.652	C_{17}-C_{18}(2)	0.361	94.73
			C_{19}-C_{22}(2)	0.335	71.96
n- π *	LPO13(2)	1.837	C_2-C_7(2)	0.387	121.84
n- σ*	LPO14(2)	1.877	C_3-C_4	0.071	100.17
			C_4-C_5	0.064	95.90
n- π *	LPO15(2)	1.838	C_3 –C_8(2)	0.468	152.30
n- π *	LPO27(2)	1.869	C_{20}-C_{24}(2)	0.394	127.32
n- π *	LPO34(2)	1.895	C_{29}-O_{35}	0.064	68.87
n- π *	LPO35(2)	1.827	C_{10}-C_{11}(2)	0.429	121.17
			C_{29}-O_{34}	0.059	54.10
			C_{29}-H $_{67}$	0.031	18.16
n- σ*	LPO36(2)	1.930	C_{31}-C_{33}	0.051	28.58
			C_{32}-C_{33}	0.046	26.07
			O_{38}-H_{39}	0.025	18.16
n- σ*	LPO38	1.972	C_{31}-C_{33}	0.051	12.30
n- σ*	LPO38(2)	1.937	C_{30}-C_{31}	0.044	26.57
			C_{31}-H_{64}	0.026	10.96
			O_{48}-H_{49}	0.029	32.13
n- σ*	LPO40(1)	1.949	C_{30}-H_{59}	0.025	13.18
			O_{36}-H_{37}	0.019	12.59
			C_{41}-O_{46}	0.041	11.25
			C_{41}-H_{47}	0.044	13.93
n- σ*	LPO40(2)	1.913	C_{29}-C_{30}	0.059	35.56
			C_{41}-C_{42}	0.064	28.70
			C_{41}-O_{46}	0.041	18.45
n- σ*	LPO46	1.949	O_{40}-C_{41}	0.048	15.82
			C_{41}-C_{42}	0.064	16.48

			C_{44}-C_{45}	0.038	14.77
n- σ*	LPO46(2)	1.914	O_{40}-C_{41}	0.048	14.39
			C_{41}-C_{42}	0.064	11.51
			C_{41}-H_{47}	0.044	36.36
			C_{44}-H_{60}	0.025	10.50
			C_{44}-C_{69}	0.026	24.81
n- σ*	LPO48	1.970	C_{42}-H_{63}	0.030	13.89
			O_{50}-H_{51}	0.016	11.59
n- σ*	LPO48(2)	1.947	C_{41}-C_{42}	0.064	39.83
			C_{42}-H_{63}	0.030	12.72
n- σ*	LPO50	1.974	C_{42}-C_{43}	0.048	8.74
n- σ*	LPO50(2)	1.952	C_{42}-C_{43}	0.048	24.06
			C_{43}-H_{62}	0.034	30.88
			C_{43}-C_{45}	0.046	32.51
			C_{45}-H_{61}	0.032	24.23
			C_{54}-H_{57}	0.030	29.66
			C_{54}-H_{58}	0.026	27.07
π*-π*	C3-C8*(2)	0.468	C-O_{14}*(2)	0.160	481.33
π*-π*	C20-C24*(2)	0.394	C_{17}-C_{18}*(2)	0.361	1107.92

[a]$E^{(2)}$ means energy of hyper conjugative interaction (stabilization energy, converted as 1kcal/mol=4.18kJ/mol),

Hyperpolarizability calculations

The first hyperpolarizabilities (β0) polarizability (α0) and dipole moment (μ) of Naringin molecule has calculated by B3LYP level of theory using 6-31G (d, p) basis set, based on the finite-field approach. In the presence of an applied electric field, the energy of a system is a function of the electric field. First hyperpolarizability is a third rank tensor that can be described by a 3x3x3 matrix. The 27 components of the 3D matrix can be reduced to 10 components due to Kleinman symmetry [42]. It can be given in the lower tetrahedral format. It is obvious that the lower part of the 3x3x3matrix is a tetrahedral. The components of β are defined as the coefficients in the Taylor series expansion of the energy in the external electric field. When the external electric field is weak and homogeneous, this expansion becomes:

$$E = E^0 - \mu_\alpha F_\alpha - 1/2\alpha_{\alpha\beta}F_\alpha F_\beta - 1/6\beta_{\alpha\beta\gamma}F_\alpha F_\beta F_\gamma \quad (3)$$

where E^0 is the energy of the unperturbed molecules, F_α is the field at the origin, and $\mu_\alpha, \alpha_{\alpha\beta}, \beta_{\alpha\beta\gamma}$ is the components of the dipole moment, polarizability and the first hyperpolarizability, respectively. The total static dipole moment μ, the mean polarizability α_0, the anisotropy of polarizability Δα and the mean first hyperpolarizability β_0, using the x, y, z components are defined as

$$\mu = \left(\mu_x^2 + \mu_y^2 + \mu_z^2\right)^{1/2} \quad (4)$$

$$\alpha_0 = \frac{\alpha_{xx} + \alpha_{yy} + \alpha_{zz}}{3} \quad (5)$$

$$\Delta\alpha = 2^{-1/2}\left[\left(\alpha_{xx} - \alpha_{yy}\right)^2 + \left(\alpha_{yy} - \alpha_{zz}\right)^2 + \left(\alpha_{zz} - \alpha_{xx}\right)^2 + \left(\alpha_{xy}^2 + \alpha_{yz}^2 + \alpha_{xz}^2\right)\right]^{1/2} \quad (6)$$

$$\beta_0 = \left(\beta_x^2 + \beta_y^2 + \beta_z^2\right)^{1/2} \quad (7)$$

Many organic molecules, containing conjugated π electrons are characterized by large values of molecular first hyper polarizabilities, were analyzed by means of vibrational spectroscopy [43-46]. The intra molecular charge transfer from the donor to acceptor group through a single-double bond conjugated path can induce large variations of both the molecular dipole moment and the molecular polarizability, making IR and Raman activity strong at the same time [47].

Table 3 lists the computed dipole moment (μ), polarizability (α) and first order hyperpolarizability (β_0) as, 1.832 Debye, 0.840 x 10-30 esu and 6.477 x 10^{-30} esu, respectively. The first hyperpolarizability (β_0) of the title molecule is fifteen times higher than that of urea; hence this molecule has considerable NLO activity. In this molecule, the π-π* interaction plays a major role in intra-molecular charge transfer and hence the hyperpolarizability of the molecule being increased.

UV-Visible Spectral Studies and HOMO-LUMO Analysis

The ultraviolet absorption spectrum was obtained in the range of 200-500 nm to study the electronic properties of Naringin. The UV pattern was taken from a 10-5 molar solution of Naringin dissolved in methanol. TD-DFT calculation was performed to examine the electronic excitations within the MOs

Table 3: The electric dipole moments (μ), polarizability **(α) and** hyperpolarizability **(β_0)** values of Naringin.

Parameters	B3LYP/6-31G(d,p)
Dipole moment (μ)	**Debye**
μ_x	-1.774
μ_y	-0.165
μ_z	0.423
μ	**1.832**
Polarizability (α)	***x10^{-30} esu***
α_{xx}	396.795
α_{xy}	-40.462
α_{yy}	362.008
α_{xz}	6.148
α_{yz}	18.176
α_{zz}	246.065
α	0.840
Hyperpolarizability (β_0)	***x10^{-30} esu***
β_{xxx}	-790.564
β_{xxy}	-511.101
β_{xyy}	210.872
β_{yyy}	49.444
β_{xxz}	-84.623
β_{xyz}	50.617
β_{yyz}	-14.420
β_{xzz}	4.864
β_{yzz}	-8.700
β_{zzz}	-2.629
β_0	6.477
Standard value for urea (μ=1.3732 Debye, β0=0.3728x10-30 esu)	

of Naringin. The both experimental UV and computed results are listed in Table 4. In this work the observed band gaps are about 328.00, 282.60, 279.80 nm and computed band gap are about 344.74, 293.04, 279.63 nm. These values clearly denote that the excitation lay among the conjugative bonds. The Figure 4 shows the absorption spectrum (in methanol) of Naringin. The frontier molecular orbitals are shown in Figure S1 (Supplementary information). The HOMO is located over the 2px orbitals of carbon and oxygen atom in ring D, E and LUMO states appears in ring A. In addition to that the neighboring HOMO-1,-2,-3 and LUMO+1, +2+3 are also shown in Figure S1. The estimated HOMO energy is -5.869 eV, and LUMO energy is -1.034 eV and the HOMO-LUMO energy gap is -4.835 eV.

Summary and Conclusion

In the present investigation we investigate the structural, spectral and molecular orbitals (MO's) properties of naringin. Naringin consists of naringenin (ring A-C), D-glucose (ring D) and L-rhamnose (ring E). The molecular geometry was studied and found the intra molecular hydrogen bonding between carbonyl and hydroxyl group (C_4=O_{14} ...H_{16}-O_{15}). Vibrational behavior of Naringin was studied by FT-IR and FT-Raman spectra, these spectral values were compared with computed vibrational wavenumbers, agreement is good and discussed the discrepancies among wavenumbers. Furthermore, inter and intra molecular charge transfers were measured by NBO analysis, this analysis clearly showed the maximum energy exchange occurs among π-π* interactions. The calculated first order hyperpolarizability ($6.477x10^{-30}$ esu) is fifteen times higher than that of urea; hence this molecule has a considerable nonlinear optical property. The obtained UV spectrum show excitations at 328.00, 282.60, 279.80 nm, this clearly denotes the excitation lay among the conjugative bonds and calculated HOMO is located over the 2px orbitals of carbon and oxygen atom in ring D, E and LUMO states appears in ring A, whereas, the band gap energy has calculated as -4.835 eV.

Table 4: The electronic transition of Naringin using TD-B3LYP/6-31G(d,p) level.

Calculated at B3LYP/ 6-31G(d,p)	Oscillator strength	Experimental Band gap (nm)	Calculated Band gap (eV/nm)
Excited state 1	Singlet-A/f=0.0010	328.00	3.5964 eV /344.74nm
151->154 ($HOMO_{-2}$-LUMO)			-5.203
153->154 (HOMO- LUMO)			-4.835
Excited State 2	Singlet-A /f=0.0499	282.60	4.2310 eV /293.04 nm
150 ->154($HOMO_{-3}$- LUMO)			-5.263
150 ->156($HOMO_{-3}$- $LUMO_{+2}$)			-6.153
150 ->157($HOMO_{-3}$- $LUMO_{+3}$			-5.939
152 ->154($HOMO_{-1}$-LUMO			-4.917
153 ->154(HOMO-LUMO			-4.835
Excited State 3	Singlet-A/ f=0.0252	279.80	4.4338 eV /279.63 nm
151 ->154($HOMO_{-2}$- LUMO)			-5.203
152 ->154($HOMO_{-1}$-LUMO)			-4.917
153 ->154(HOMO-LUMO)			-4.835

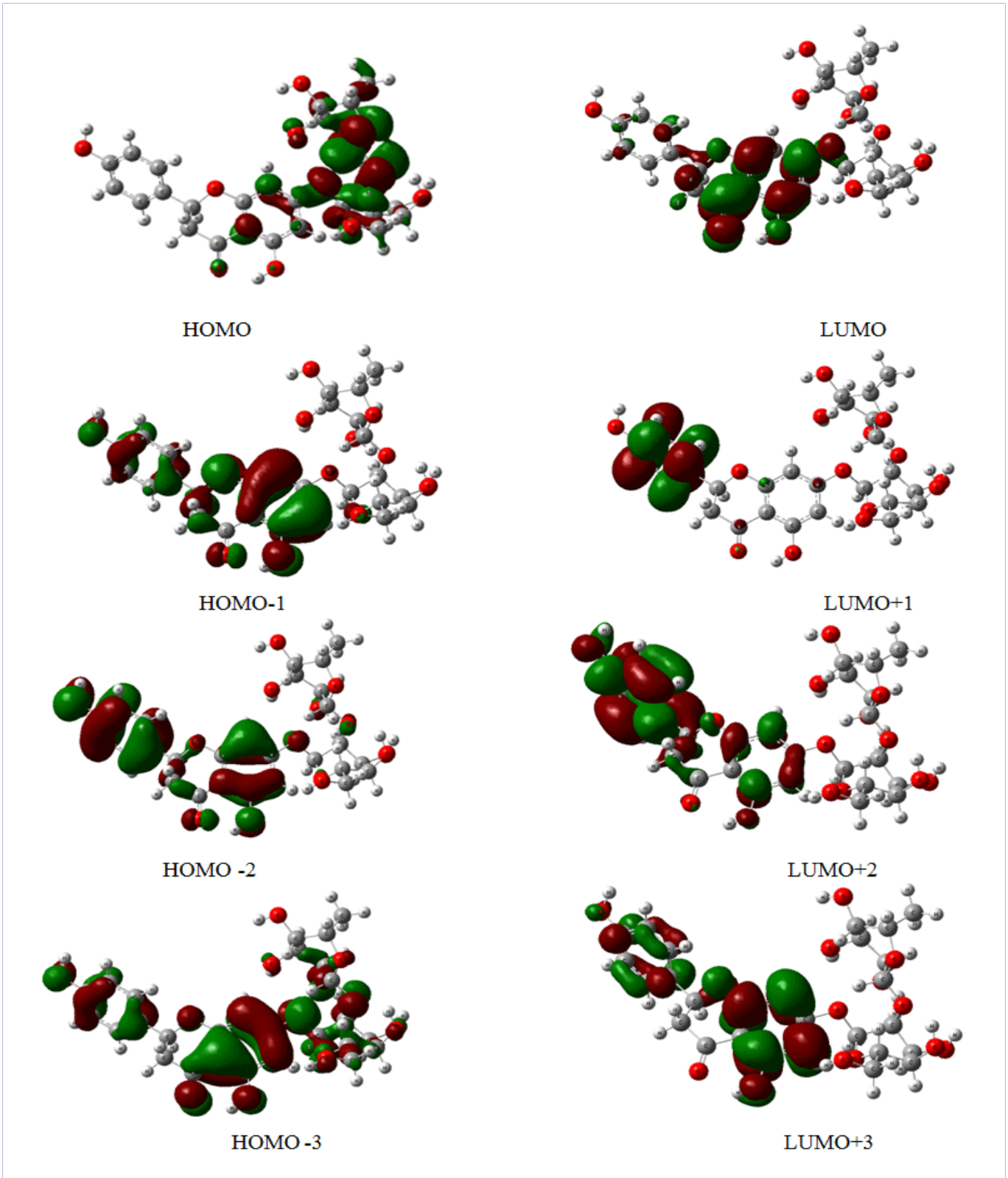

Figure S1: The Frontier molecular orbitals of Naringin.

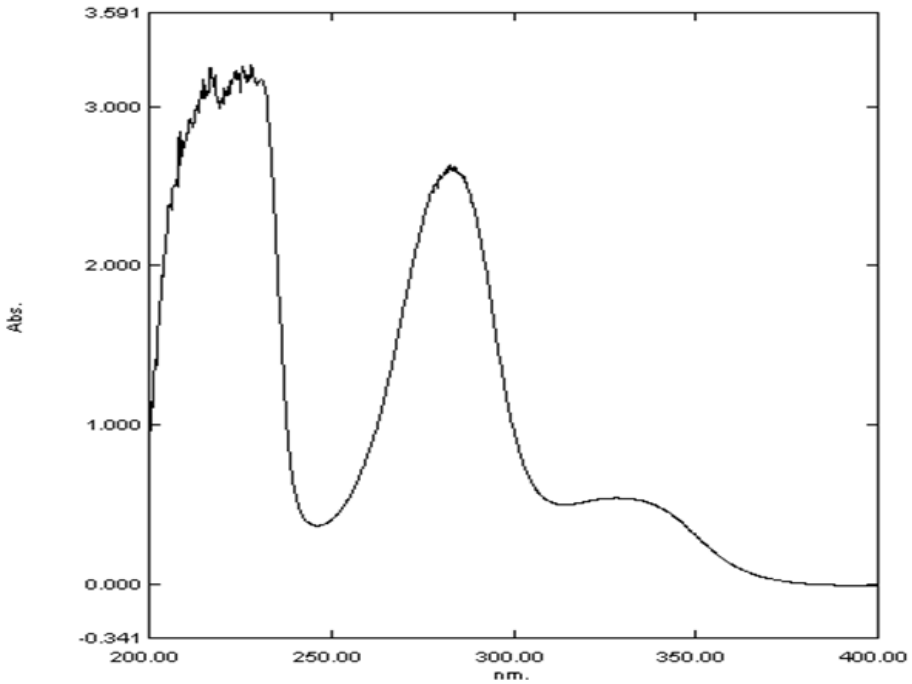

Figure 4: The UV-Visible spectrum is taken from a 10-5 molar solution of Naringin dissolved in methanol.

References

1. Cook NC and Samman S. Flavonoids—Chemistry, metabolism, cardioprotective effects, and dietary sources. J Nutr Biochem. 1996;7(2):66–76.

2. Ribeiro MH. Naringinases: occurrence, characteristics, and applications. Appl Microbiol Biotechnol. 2011;90(6):1883–1895. Doi: 10.1007/s00253-011-3176-8.

3. Renugadevi J and Prabu SM. Naringenin protects against cadmium-induced oxidative renal dysfunction in rats. Toxicology. 2009;256(1-2):128–134.

4. Choudhury R, Chowrimootoo G, Srai K and Debnam E, Rice-Evans CA. Interactions of the Flavonoid Naringenin in the Gastrointestinal Tract and the Influence of Glycosylation. Biochem Biophys Res Commun. 1999;265(2):410–415.

5. Parini M, Braquet P and Garany RP. Heterogenous effect of flavonoids on K+ loss and lipid peroxidation induced by oxygen-free radicals in human red cells. Pharmacol. Res. Commun. 1986;18(1) 61-72.

6. Jung G. Hennings G, Pfeifer M, and BesslerWG. Iteraction of metal-complexing coumpounds with lymphocytes and lympho cell lines. Mol. Pharmacol. 1983;23(3):698-702.

7. Jagetia GC, Venkatesha VA and Reddy TK. Naringin, a citrus flavonone, protects against radiation-induced chromosome damage in mouse bone marrow. Mutagenesis. 2003;13(4):337-343.

8. Schindler R and Mentlein R. Flavonoids and vitamin E reduce the release of the angiogenic peptide vascular endothelial growth factor from human tumor cells. J. Nutr. 2006;136(6):1477-1482.

9. Martin MJ, Marhuenda E, Perez-Guerrero C and Franco JM. Antiulcer Effect of Naringin on Gastric Lesions Induced by Ethanol in Rats. Pharmacology. 1994;49(3):144-150.

10. Gaussian 03 program, (Gaussian Inc., Walling ford CT) 2004.

11.Schlegel HB. Optimization of equilibrium geometries and transition structures J. Comput. Chem. 1982;3(2):214-218.

12.Frisch NAB and Holder AJ. GAUSSVIEW User Manual, Gaussian Inc, Pittsburgh PA. 2000.

13.Rauhut G and Pulay G. Transferable Scaling Factors for Density Functional Derived Vibrational Force Fields. J. Phys. Chem. 1995;99(10):3093-3100.

14.Michalska D. Raint Program. Wroclaw University of Technology.2003.

15.Michalska D and Wysokinski R. The prediction of Raman spectra of platinum(II) anticancer drugs by density functional theory. Chem. Phys. Lett. 2005;403(1-3):211-217.

16.Wera M, Serdiuk LE, Roshal AD and Jerzy B. ejowski . 3-Hydroxy-2-(4-methoxyphenyl)-4Hchromen-4-one J. Blazejowski. Acta Cryst. 2011;E67(o440).

17.Zhang ZT and Zhang XL. F-type or T-type Aromatic–Aromatic Interaction in Two Isoflavone Derivatives. J. Chem. Crystallogr. 2008;38(2):129-133.

18.Silverstein M, Basseler CG and Morill CT. Spectrometric Identification of Organic Compounds. Wiley: New York, 1981.

19.Krishnakumar V, Murugeswari K, Prabavathi N and Mathammal R. Molecular structure, vibrational spectra, HOMO, LUMO and NMR studies of 2-chloro-4-nitrotoluene and 4-chloro-2-nitrotoluene. Spectrochim. Acta A. 2012;91:1-10.

20.Varsanyi G. Vibrational Spectra of Benzene Derivatives. Academic Press: New York. 1969.

21.Colthup NB, Daly LH and Wiberly SE. Introduction to Infrared and Raman spectroscopy. Academic Press: New York. 1990.

22.Erdoğdu Y and Güllüoglu MT. Analysis of vibrational spectra of 2 and 3-methylpiperidine based on density functional theory calculations. Spectrochim. Acta. 2009;74(1):162-167.

23.Roeges NPG. A Guide to the Complete Interpretation of Infrared Spectra of Organic Structures. Wiley: New York.1994.

24.Varghese HT, Paniker CY, Madhavan VS, Mathew S, Vinsova J and Alsenoy CV. FT-IR, FT-Raman and DFT calculations of the salicylanilide derivate 4-chloro-2-(4-bromophenylcarbamoyl)phenyl acetate. J. Raman. Spectrosc. 2009;40(9):1211-1223.

25.Sundaraganesan N, Meganathan C, Saleem H and Dominic Joshua B. Vibrational spectroscopy investigation using ab initio and density functional theory analysis on the structure of 5-amino-o-cresol. Spectrochim. Acta A. 2007;68(3):619-625.

26.Sebastien S and Sundaraganesan N. The spectroscopic (FT-IR, FT-IR gas phase, FT-Raman and UV) and NBO analysis of 4-Hydroxypiperidine by density functional method. Spectrochim. Acta A. 2010;75(3):941-952.

27.Ramalingam M, Joccob M, Venuvanlingam P and Sundaraganesan N. Harmonic analysis of vibrations of morpholine-4-ylmethylthiourea: A DFT, midinfrared and Raman spectral study. Spectrochim. Acta A. 2008;71(3):996-1002.

28.Pavia DL, Lampman GM and Kriz GS. Introduction to Spectroscopy. Third Edition, Thompson Learning, US. 2001.

29.Oliveira RN, Mancini MC, Oliveira FCS, Passos TM, Quility B and Thiré B, et. al. FTIR analysis and quantification of phenols and flavonoids of five commercially available plants extracts used in wound healing. Revista Matéria. 2016;21(3):767–779.

30.Akkaya Y and Akyüz S. Infrared and Raman spectra, ab initio calculations vibrational assignment of 4-aminosalicylic acid. Vib. Spectrosc. 2006;42(2):292-301.

31.Nogueira HIS. Surface-enhanced Raman scattering (SERS) of 3-aminosalicylic and 2-mercaptonicotinic acids in silver colloids. Spectrochim. Acta A. 1998;54(10):1461-1470.

32.Sundaraganesan N, Meganathan C, Anand B and Lapouge C. FT-IR, FT-Raman spectra and ab initio DFT vibrational analysis of p-bromophenoxyacetic acid. Spectrochim. Acta A. 2007;66(3):773-780.

33.Erdoğdu Y, Unsalan O and Güllüoglu MT. FT-Raman, FT-IR spectral and DFT studies on 6, 8-dichloroflavone and 6, 8-dibromoflavone. J. Raman Spectrosc. 2010;41(7):820-828.

34.Puri M, Kurt A, Schwarz WH, Singh S and Kennedy JF. Molecular characterization and enzymatic hydrolysis of naringin extracted from kinnow peel waste. Int. J. Bio. Macromol. 2011;48(1):58-62.

35.Subramanian MK, Anbarasan PM and Manimegali S. Molecular structure, NMR and vibrational spectral analysis of 2,4-difluorophenol by ab initio HF and density functional theory. J. Raman Spectrosc. 2009;40(11):1657-1663.

36.Ficarra R, Tommasini S, Raneri D, Calabrò ML, Di Bella MR and Rustichelli C, et. al. Study of flavonoids/beta-cyclodextrins inclusion complexes by NMR, FT-IR, DSC, X-ray investigation. J Pharm Biomed Anal. 2002;29(6):1005-1014

37.Reed AE, and Weinhold F. Natural bond orbital analysis of near-Hartree–Fock water dimer. J. Chem. Phys. 1983;78(6):4066-4073.

38.Reed AE, and Weinhold F. Natural localized molecular orbitals. J. Chem. Phys. 1985;83(4):1736-1740.

39.Reed AE, Weinstock RB and Weinhold F. Natural population analysis. J.Chem. Phys. 1985;83(2):735-746.

40.Foster JP and Wienhold F. Natural hybrid orbitals. J. Am. Chem. Soc. 1980;102(24):7211-7218.

41.Chocholousova J. Vladimir Spirko J and Hobza P. First local minimum of the formic acid dimer exhibits simultaneously red-shifted O–H···O and improper blue-shifted C–H···O hydrogen bonds. Phys. Chem. Chem. Phys. 2004;6(1):37-41.

42.Colthup NB, Daly LH and Wiberly SE, Introduction to Infrared and Raman Spectroscopy. Academic Press: New York, 1990.

43.Castiglioni C, Del zoppo M, Zuliani P and Zerbi G. Experimental molecular hyperpolarizabilities from vibrational spectra in systems with large electron-phonon coupling. Synth. Met. 1995;74(2):171-177.

44.Del zoppo M, Castiglioni C and Zerbi G, Non-Linear Opt. 1995;9:73.

45.Del zoppo M, Castiglioni C, Zuliani P, Razelli A, Zerbi G and Blanchard-Desce M. Use of vibrational spectra for the determination of first-order molecular hyperpolarizabilities of push–pull polyenes as function of structural parameters. J. Appl. Polym. Sci. 1998;70(7):1311-1320.

46.Zuliani P, Del zoppo M, Castiglioni C and Zerbi G. Solvent effects on first-order molecular hyperpolarizability: A study based on vibrational observables. Chem. Phys. 1995;103(23):9935.

47.Ravikumar C, Huber Joe I and Jayakumar VS, Charge transfer interactions and nonlinear optical properties of push–pull chromophore benzaldehyde phenylhydrazone: A vibrational approach. Chem. Phys. Lett. 2008;460(4-6):552-558.